Global variations of surface ocean productivity in low and mid latitudes: influence on C0_2 reservoirs of the deep

Michael Sarnthein, Kyaw Winn, Jean-Claude Duplessy, Michael Fontugne

▶ **To cite this version:**

Michael Sarnthein, Kyaw Winn, Jean-Claude Duplessy, Michael Fontugne. Global variations of surface ocean productivity in low and mid latitudes: influence on C0_2 reservoirs of the deep. Paleoceanography, 1988, 3 (3), pp.361-399. 10.1029/PA003i003p00361 . hal-03543888

HAL Id: hal-03543888
https://hal.science/hal-03543888

Submitted on 26 Jan 2022

HAL is a multi-disciplinary open access archive for the deposit and dissemination of scientific research documents, whether they are published or not. The documents may come from teaching and research institutions in France or abroad, or from public or private research centers.

L'archive ouverte pluridisciplinaire **HAL**, est destinée au dépôt et à la diffusion de documents scientifiques de niveau recherche, publiés ou non, émanant des établissements d'enseignement et de recherche français ou étrangers, des laboratoires publics ou privés.

PALEOCEANOGRAPHY, VOL. 3, NO. 3, PAGES 361-399, JUNE 1988

GLOBAL VARIATIONS OF SURFACE OCEAN PRODUCTIVITY IN LOW AND MID LATITUDES: INFLUENCE ON CO_2 RESERVOIRS OF THE DEEP OCEAN AND ATMOSPHERE DURING THE LAST 21,000 YEARS

Michael Sarnthein and Kyaw Winn

Geologisch-Paläontologisches Institut
Christian-Albrechts-Universität
Kiel, Federal Republic of Germany

Jean-Claude Duplessy and
Michel R. Fontugne

Centre des Faibles Radioactivites
Gif-sur-Yvette, France

Abstract. Based on detailed reconstructions of global distribution patterns, both paleoproductivity and the benthic $\delta^{13}C$ record of CO_2, which is dissolved in the deep ocean, strongly differed between the Last Glacial Maximum and the Holocene. With the onset of Termination I about 15,000 years ago, the new (export) production of low- and mid-latitude upwelling cells started to decline by more than 2-4 Gt carbon/year. This reduction is regarded as a main factor leading to both the simultaneous rise in atmospheric CO_2 as recorded in ice cores and, with a slight delay of more than 1000 years, to a large-scale gradual CO_2 depletion of the deep ocean by about 650 Gt C. This estimate is based on an average increase in benthic $\delta^{13}C$ by 0.4-0.5‰. The decrease in new production also matches a clear ^{13}C depletion of organic matter, possibly recording an end of extreme nutrient utilization in upwelling cells. As shown by Sarnthein et al., [1987], the productivity reversal appears to be triggered by a rapid reduction in the strength of meridional trades, which in turn was linked via a shrinking extent of sea ice to a massive increase in high-latitude insolation, i.e., to orbital forcing as primary cause.

Copyright 1988
by the American Geophysical Union.

Paper number 8P0310.
0883-8305/88/008P-0310$10.00

INTRODUCTION

Measurements of gases trapped in polar ice cores [Delmas et al., 1980; Neftel et al., 1982; Oeschger et al., 1984; Barnola et al., 1987] convincingly demonstrated that the concentration of atmospheric carbon dioxide was subject to several dramatic natural changes which paralleled and possibly slightly preceded the major climatic fluctuations between and during glacial and interglacial stages of the last 160,000 years. Since the ocean contains about 60 atmospheric carbon units [e.g., Grassl et al., 1984; Sundquist, 1985], any such change of atmospheric pCO_2 must be tied to the ocean and requires a large-scale redistribution of the ocean chemical properties [e.g., Broecker and Takahashi, 1984]. First evidence for this change in the ocean was observed by Shackleton [1977] and Duplessy [1982] in the $\delta^{13}C$ composition of benthic foraminifera. The evidence of Oeschger et al. [1984] and Barnola et al. [1987] even suggests that the carbon redistribution may have proceeded very rapidly, implying that most of the pCO_2 changes in the atmosphere possibly took place within a time span as short as a few centuries or less during early deglacial times. Also, much slower changes cannot be explained by the insufficient effect of an average temperature

increase of the surface ocean or by a sedimentation pulse of nutrients bound in organic matter on the continental shelves during the transgression at the end of glacial time [Broecker, 1982]. The storage of C, N, and P on the shelves slowly started during this transgression, while the atmospheric pCO_2 was already high. Other mechanisms must therefore be invoked [Broecker, 1984; Dymond and Lyle, 1985].

A large number of ocean-atmosphere models have been used to explore the causes for these CO_2 fluctuations [see Sundquist and Broecker, 1985]. The background reasoning and assumptions in many of these models have been summarized by Berger and Keir [1984], Broecker and Takahashi [1984], Broecker and Peng [1986], and Sundquist [1985]. Unfortunately, most of the models are backed up by little hard data.

Besides a minor but certain input from lowering the forest biomass [Shackleton, 1977], there remain, basically, two main options for decreasing the pCO_2 in the atmosphere through increasing CO_2 in the main reservoir of the deep ocean such as during the last glaciation. One choice is to reduce the production and turnover of deep water, in particular, that of North Atlantic Deep Water (NADW) in high latitudes. Such a change will result in a more sluggish deep-ocean circulation. Once the exchange rate of deep water diminishes, the oxygen supply from the high-latitudinal surface water is likely to become reduced. More particulate organic carbon and nutrients (in order to keep the Redfield ratio C:N:P = 106:16:1 constant, Takahashi et al., [1985]) will be stored in deep water over long time spans, and accordingly, more CO_2 can be extracted from the surface ocean and the atmosphere [Duplessy, 1982; Duplessy and Shackleton, 1985; Oeschger et al., 1984; Broecker et al., 1985]. Broecker et al. [1984] and Broecker [1987] provided the first evidence from accelerator radiocarbon-dated foraminifera that indeed the glacial deep ocean, especially the Atlantic, was more sluggish than it is today.

A mechanism along this line still contains a number of basic problems. According to the model of Broecker and Takahashi [1984], it was not the deep water ventilation of the ocean only, but the ratio between it and the CO_2 gas exchange rate between the air and the sea, that controls the different CO_2 budgets (when excluding, for simplification, the role of carbon and nutrient transfer with particulate organic matter in high latitudes). In this case, simply an increase of oceanic ventilation and a decrease of gas exchange would result in leading to the glacial lowering of atmospheric CO_2 ("Redfield Ocean"). This model now appears less plausible in view of the recent results of Broecker [1987].
The second option for decreasing atmospheric CO_2 is to assume a considerable increase in the flux rate of particulate carbon across the thermocline during glacial time, along with a decrease in the preformed nutrient content of the downwelled deep water that formed in the high-latitudinal oceans [Oeschger et al., 1984]. However, Mix and Fairbanks [1985] suggested that there was an increase of the preformed nutrient content of synglacial deep water because, in part, it possibly formed below sea-ice cover, an assumption we don't necessarily follow [Duplessy et al., 1988]. This second option implies that the synglacial new (or "export") primary production of the ocean was especially enhanced in the mid and low latitudes, whereas it was largely reduced in the higher latitudes as a result of expanded sea-ice cover. The high synglacial productivity in low latitudes, in turn, required a strongly enhanced lateral advection of nutrients to low-latitudinal upwelling regions, a transport which today takes place mainly in intermediate waters (upper 200-700 m). This turnover of intermediate waters has to be considered as decoupled from that of the deep water of the ocean because it originates from different downwelling zones. Hence it can cause a large-scale nutrient redistribution, which bypasses the deep ocean and fuels the little used nutrient reservoir of the high-latitude surface ocean to the warm low latitudes where the nutrients become almost completely fixed in organic tissues. Complementary to this mechanism, changes in the C:P (Redfield) ratio may be a possible cause for such a high-productivity scenario as theoretically considered by Broecker [1982] and demonstrated by M. Sarnthein and T. Takahashi [unpublished manuscript, 1988].

Based on modern oceanographic data, Newell et al. [1978], Newell and Hsiung [1984], and Flohn [1982] were the first to suggest that variations in low-latitude upwelling may be crucial in controlling

atmospheric pCO_2. They related this forcing to the combined effect of lowering the sea surface temperature (SST) and increasing productivity and carbon extraction from the surface water. Based on direct observations in the equatorial Atlantic, Garcon et al. [1986] regard the biological CO_2 uptake as a more crucial constraint on the nutrient balance of the equatorial divergence than gas fluxes. Siegenthaler and Wenk [1984], unlike Wenk and Siegenthaler [1985], presented a glacial CO_2 model, which includes this option of enhancing the particulate carbon transfer by biological activity in both high and low latitudes. To reach this target, they had to allow for an increased utilization of the surface water nutrient pool during the ice age. They assumed a simultaneous general reduction of preformed nutrients in the deep water as a result of biologically induced stronger nutrient depletion in the high-latitude downwelling regions. Like us, they considered this nutrient distribution to be the result of enhanced near-surface circulation and included upwelling in low latitudes as a major factor controlling the particulate carbon transfer.

Vincent and Berger [1985] specified the effects of low-latitudinal upwelling more explicitly in their "Monterey" hypothesis to explain the middle Miocene CO_2 shift. Their approach includes a further important concept, the "Rain-Ratio" model of Berger and Keir [1984]. According to this model, for the particle flux crossing the thermocline the "rain" of carbonate carbon and organic carbon have an opposing effect on CO_2 balance. With increasing fertility this Rain Ratio will shift substantially towards organic carbon and thereby strongly increase the total CO_2 dissolved in the deep ocean. Indirect support for this concept comes from the findings of Eppley and Peterson [1979], who showed that the proportion of new production out of the total plankton production increases markedly from about 6 to 50% when going from low- to high-productivity regions. Based on this reasoning, Dymond and Lyle [1985] developed a three-box ocean model, which explicitly relates the required short-term changes in the extraction of atmospheric carbon to possible fluctuations of low- and mid-latitudinal primary production, which in turn is controlled by wind-driven upwelling. Hence high rates of new production may be triggered rapidly, and synchronously, over wide parts of the ocean. Based on data from empirical paleoproductivity curves from the east Atlantic, Müller et al. [1983] and Sarnthein et al. [1987] arrived at a similar conclusion. Indeed, zonal sea surface temperature anomalies show that the average intensity of wind-driven coastal upwelling along the (north-) east Atlantic continental margin increased by at least 50% during the Last Glacial Maximum (LGM)[Sarnthein, 1982]. Recently, Boyle [1986a] presented a CO_2 model of the ocean and the atmosphere, which relies on wind-driven low-latitude upwelling productivity. However, this model can only explain 1/3-1/4 (about 25 parts per million by volume) of the observed atmospheric pCO_2 change during the last deglaciation.

In this paper we try to evaluate the contribution of the "second option" to the last glacial-to-interglacial change in pCO_2 by two new, but still preliminary and small, global sets of empirical data. We compare the sedimentary record of surface ocean paleoproductivity with the benthos carbon isotope record of dissolved CO_2 in the deep water from the various ocean basins during the LGM, glacial Termination I, and the Recent. For calculating paleoproductivity from sediments we utilize an empirical equation (improved version of Sarnthein et al. [1987], based on concepts of Müller and Suess [1979] and Suess [1980]). Since we cannot present a complementary set of global variations in $CaCO_3$ production and dissolution, our conclusions on fluctuations of the atmospheric and oceanic CO_2 budget have to rely strongly on the premises of the Berger and Keir [1984] Rain-Ratio model.

Furthermore, we discuss some possible signals of productivity stress on the nutrient and carbon reservoirs in the surface waters during times of extreme nutrient utilization, i.e., a possible environmental response to the proposed large-scale carbon extraction. Finally, we test the different options for a carbon enrichment of the deep ocean by a global survey of the leads and lags of the $\delta^{18}O$ deglaciation signal versus changes of paleoproductivity and bottom water oxygenation during the special case of Termination I. From this we expect a better understanding of the cause and effect relationships and possible feedback loops during times of rapid climatic change.

METHODS

Values of ancient new primary production of organic carbon ("new paleoproductivity" = P_{new}) were derived from deep-sea sediments using equation (1)

$$P_{new} = 0.0238 * C^{0.6429} * S_B^{0.8575} * DBD^{0.5364} * z^{0.8292} * S_{B-C}^{-0.2392} \quad (g\ m^{-2}\ yr^{-1}) \quad (1)$$

where C is the concentration of organic carbon, DBD is the dry bulk density, S_B the bulk sedimentation rate, S_{B-C} the (organic) carbon-free sedimentation rate, and z the water depth. The carbon concentrations in the sediment cores were measured at 1- to 2-cm-thick samples at 10 cm and smaller downcore intervals by means of both Leco^R and Coulomat 702^R instruments, and by mass spectrometry [Gif-sur-Yvette].

The principles underlying equation (1) were discussed in detail by Sarnthein et al. [1987]. The equation is based on the assumption that the carbon accumulation rate is mainly a function of primary production, water depth (according to equation (3)), and of the (carbon-free) sedimentation rates acting as "sealing factor," which comprises various processes of carbon degradation near the sediment surface (see below).

In the present paper the original equation of Sarnthein et al. [1987] was slightly modified and improved. First, we included the nonlinear positive relationship between total primary production (P_{tot}) and new (=export) production (P_{new}) as described by Eppley and Peterson [1979]:

$$P_{new} = P_{tot}^2 / 400 \quad (2)$$

$$(P_{new} = P_{tot}/2 \text{ at } P_{tot} > 200\ g\ m^{-2}\ yr^{-1})$$

This modification is important because P_{new}, not P_{tot}, is controlling the extraction of CO_2 from the sea surface. Second, we nearly doubled the sediment trap data base (from 38 to 67 data points) for calculating the relationship between P_{new}, carbon flux near the seafloor F_C, and water depth (Table 1, Figure 1a) (equation (3)).

$$F_C = 20.5631 * P_{new}^{0.6648} * z^{-0.5537} \quad (3)$$

$$(r = 0.92)$$

Furthermore, the data matrix for the original paleoproductivity equation was supplemented with data from 18 Pacific and Indian Ocean sediment samples in order to enlarge its calibration base (Table 2, Figure 1b). Finally, the complete data set derived from modern sediment samples and modern new productivity estimates (equation (4)) was subjected to a linear multiple regression analysis with total forcing resulting in equation (1).

$$P_{new} * z^{-0.8292} = f\ (C,\ S_B,\ DBD,\ S_{B-C}) \quad (4)$$

Measured (and calculated) P_{new} values and the P_{new} estimates from equation (1) agree with a correlation coefficient of $r = 0.84$ ($n = 57$) (Figure 1b).

We are aware that this empirical equation presents an attempt to deduce one of the most important variables of the ocean, paleoproductivity, from a deposit that constitutes, on the average, less than 0.5-2.0% of the carbon originally produced. Nevertheless, a test run of the equation employing modern sediment data [Sarnthein et al., 1987] provided satisfactory results and strongly encouraged its application to the fossil record. Furthermore, the paleoproductivity trends we find are corroborated by parallel fluctuations in the accumulation rates of biogenic silica, which are available in a few cases (e.g., from the south Indian Ocean, and the eastern equatorial Atlantic and Pacific; Pichon et al. [1987]; Thiede et al. [1982]; Lyle et al. [1988]).

The equation itself still contains a number of pitfalls and major generalizations, including the following:

1. Many of the values of modern primary productivity we used for equation (1) were derived from Koblentz-Mishke et al. [1970] (improved version from FAO [1981]) who measured them by the principle of C-14 assimilation, a method which has recently been criticized [Jenkins, 1982; Platt and Harrison, 1985]. Many authors claim that this method understimates productivity; other authors rather see the conventional C-14 estimates confirmed (see review in the work of Brewer et al. [1986]).

2. The relationship between P_{tot} and P_{new} proposed by Eppley and Peterson [1979] may require further refinement and an enlarged data base. However, as shown by the careful studies of Betzer et al. [1984] and Bishop and Marra [1984], the F_C to P_{tot} ratio is, in principle, positively correlated to P_{tot}.

3. The relationship between the carbon fluxes near the seafloor and P_{new} has only

TABLE 1. Organic Flux Rates in the Water Column and Mean New Primary Production P_{new} Compiled From Various Sources

Latitude, °	Longitude, °	Water Depth, m	Carbon Flux, gC m^{-2} yr^{-1}	New Primary Production gC m^{-2} yr^{-1}	References
31.5 N	55.9 W	976	0.89	4.0	(a)
31.5 N	55.9 W	3694	0.32	4.0	(a)
31.5 N	55.9 W	5206	0.45	5.0	(a)
13.5 N	54.0 W	389	2.46	6.2	(a)
13.5 N	54.0 W	988	1.44	6.2	(a)
13.5 N	54.0 W	3755	0.63	6.2	(a)
13.5 N	54.0 W	5068	0.62	6.2	(a)
15.3 N	151.5 W	378	1.30	4.0	(a)
15.3 N	151.5 W	2778	0.40	4.0	(a)
15.3 N	151.5 W	4280	0.32	4.0	(a)
15.3 N	151.5 W	5582	0.24	4.0	(a)
32nm SE	Bermuda	3200	0.77	4.0	(a)
0.6 N	86.1 W	2650	2.28	25.0	(a)
27.7 N	78.9 W	675	2.60	13.0	(a)
33.5 N	76.2 W	1345	5.40	18.0	(a)
38.3 N	69.6 W	3650	4.20	64.0	(a)
24.9 N	77.7 W	2000	2.10	13.0	(a)
36.7 N	122.2 W	50	158.00	250.0	(a)
36.7 N	122.2 W	250	92.00	250.0	(a)
36.7 N	122.2 W	700	42.00	250.0	(a)
36.7 N	122.2 W	50	33.00	56.0	(a)
36.7 N	122.2 W	250	19.00	56.0	(a)
36.7 N	122.2 W	700	17.00	56.0	(a)
32.8 N	144.4 W	75	25.00	25.0	(a)
32.8 N	144.4 W	575	5.30	25.0	(a)
32.8 N	144.4 W	1050	4.40	25.0	(a)
38.8 N	72.5 W	2200	6.30	25.0	(a)
38.5 N	72.0 W	2750	2.30	64.0	(a)
55.6 N	15.4 E	55	65.00	150.0	(a)
15.1 S	75.4 W	50	240.00	600.0	(a)
15.1 S	75.5 W	70	130.00	300.0	(a)
15.1 S	75.5 W	100	110.00	300.0	(a)
6.6 N	92.8 W	500	1.45	21.3	(g)
6.6 N	92.8 W	1500	1.70	21.3	(g)
6 6 N	92.8 W	3075	1.10	21.3	(g)
8.8 N	104.0 W	2700	1.38	14.1	(g)
34.0 N	65.8 W	5140	0.72	13.0	(a)
32.5 N	117.8 W	1193	9.80	136.0	(a)
32.3 N	117.5 W	1230	9.80	136.0	(a)
32.5 N	120.6 W	3815	9.80	153.0	(a)
5.3 N	81.8 W	667	4.56	39.0	(b,f)
5.3 N	81.8 W	1268	3.28	39.0	(b,f)
5.3 N	81.8 W	2265	3.28	39.0	(b,f)
5.3 N	81.8 W	2869	3.94	39.0	(b,f)
5.3 N	81.8 W	3769	4.15	39.0	(b,f)
5.3 N	81.8 W	3791	3.84	39.0	(b,f)
50.0 N	145.0 W	1000	3.40	12.3	(g)
50.0 N	145.0 W	3800	2.25	12.3	(g)
6.0 S	153.0 W	900	2.80	107.0	(e)
0.0	153.0 W	900	3.00	114.0	(e)
6.0 N	153.0 W	900	1.65	36.5	(e)
12.0 N	153.0 W	900	0.90	7.8	(e)
51.0 N	145.0 W	250	12.40	81.0	(d)

TABLE 1. (continued)

Latitude, °	Longitude, °	Water Depth, m	Carbon Flux, gC m^{-2} yr^{-1}	New Primary Production gC m^{-2} yr^{-1}	References
51.0 N	145.0 W	600	11.50	81.0	(d)
51.0 N	145.0 W	900	9.10	81.0	(d)
51.0 N	145.0 W	1200	10.90	81.0	(d)
51.0 N	145.0 W	2000	8.20	81.0	(d)
51.0 N	145.0 W	2500	7.80	81.0	(d)
51.0 N	145.0 W	3000	6.75	81.0	(d)
60.9 N	57.0 W	965	5.41	3.3	(c)
60.9 N	57.0 W	2540	4.78	3.3	(c)
35.8 N	123.7 W	100	23.70	105.0	(h)
35.8 N	123.7 W	200	16.40	105.0	(h)
35.8 N	123.7 W	300	12.00	105.0	(h)
35.8 N	123.7 W	500	9.10	105.0	(h)
35.8 N	123.7 W	600	9.10	105.0	(h)
35.8 N	123.7 W	700	6.20	105.0	(h)

(a) See Table 1, Sarnthein et al. [1987]; (b) Honjo et al. [1982]; (c) Wefer et al. [1982]; (d) Lorenzen et al. [1983]; (e) Betzer et al. [1984]; (f) Bishop and Marra [1984]; (g) Honjo [1984]; (h) Karl and Knauer [1984].

been measured at few sediment trap locations in the world ocean running through a complete year or longer (Table 1). Recent data of Walsh et al. [1988] could no longer be incorporated in our data set. The present variability of P_{new} and the particulate carbon fluxes (F_c) may not be considered sufficiently. In general, we may assume that pulsating bloom populations dominate the export of particulate organic matter to the deep ocean.

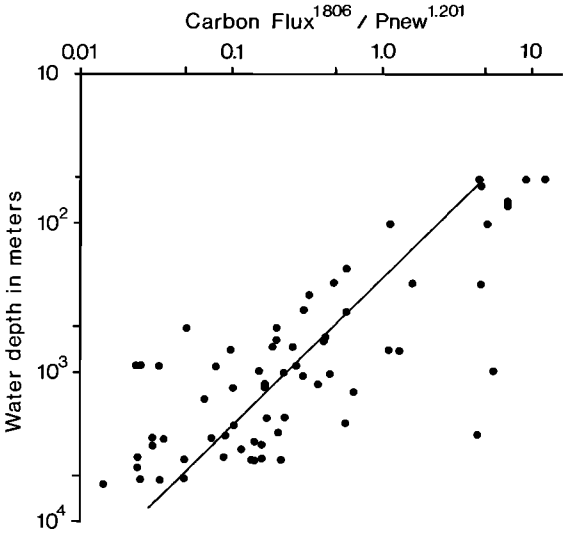

Fig. 1a. Organic carbon fluxes in water depths below 100 m at sites of sediment trap employment, normalized to annual means of new primary production. Data base in Table 1. Extremely high relative flux values are derived from Weddell Sea [Wefer et al., 1982].

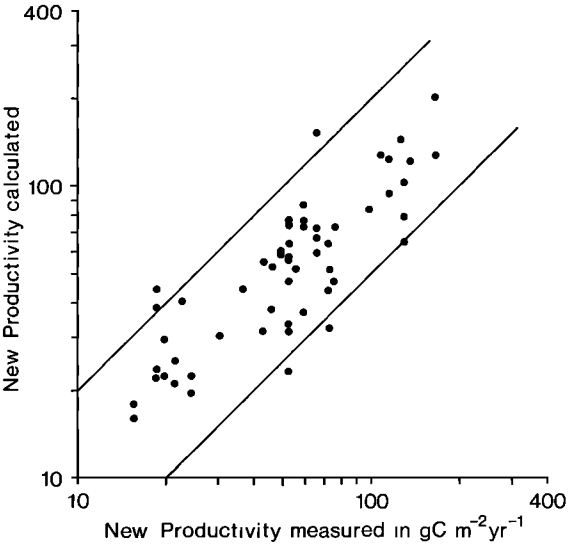

Fig. 1b. Measured values of new primary production versus estimates calculated from equation (1) based on Table 2. Bounding lines mark a deviation within a factor of 2.

TABLE 2. Core Data Used in the Derivation of Productivity Formula

Core Number or Station	Water Depth, m	C, wt %	$\rho_s(1-\phi)$, g/cc	S_B, cm/ka	S_{B-C}, cm/ka	New Production Measured, gC/m²yr	New Production Estimated, gC/m²yr
23199-1	1968	0.63	0.4190	4.50	4.47	20.3	15.2
23055-2	2308	0.55	0.5160	2.00	1.99	25.0	10.7
12392-1	2575	0.35	0.9780	5.05	5.03	14.1	22.0
12310-3	3076	0.34	0.6504	3.80	3.79	20.3	16.8
12327-4	2037	1.34	0.4065	8.33	8.22	39.1	36.6
12328-4	2798	1.66	0.5691	15.08	14.83	115.0	94.5
12329-4	3315	0.61	0.6233	2.56	2.54	36.0	20.0
12336-1	3645	0.44	0.6775	2.20	2.19	39.1	16.7
12337-4	3085	1.46	0.5691	4.90	4.83	64.0	47.1
12344-3	711	2.59	0.5691	16.45	16.02	105.0	42.7
12345-4	966	3.67	0.5691	16.45	15.85	105.0	69.1
12347-1	2710	2.34	0.5691	12.48	12.19	76.6	102.3
13209-2	4713	0.51	0.5691	3.20	3.18	18.1	26.1
13521-1	4504	0.37	0.6450	3.50	3.49	20.3	23.1
16017-2	812	1.81	0.9879	6.80	6.68	105.0	29.4
16402-1	4203	0.46	0.6037	5.24	5.22	30.3	31.1
16403-2	4234	0.45	0.6310	3.66	3.64	30.3	25.3
16404-1	4787	0.42	0.6460	3.17	3.16	18.1	24.8
16405-1	4870	0.43	0.7501	3.40	3.39	20.3	28.9
16415-1	3841	0.61	0.6500	2.70	2.68	20.3	23.9
16432-2	4515	0.52	0.6447	5.40	5.37	20.3	37.7
V15-141	5934	0.72	0.6500	2.90	2.88	25.0	39.8
V15-142	5885	0.92	0.6500	3.30	3.27	25.0	50.2
10127-2	5686	0.28	0.3710	0.19	0.19	2.3	2.9
10132-1	5004	0.22	0.5300	0.58	0.58	4.0	5.3
10140-1	5144	0.33	0.3735	0.41	0.41	3.1	4.7
10141-1	5189	0.31	0.3735	0.36	0.36	3.1	4.2
10145-1	4599	0.21	0.5300	0.32	0.32	5.1	3.3
10147-1	4619	0.23	0.5300	0.43	0.43	5.1	4.3
10175-1	5164	0.40	0.3968	0.23	0.23	4.0	3.9
7706-37	3700	13.20	0.2702	50.00	43.40	85.6	97.1
7706-39	186	13.20	0.2268	160.00	138.88	165.0	102.6
7706-41	411	19.60	0.1910	160.00	128.64	165.0	237.0
7706-44	580	7.83	0.4880	13.00	11.98	85.6	59.3
7706-49	3970	3.23	0.2300	20.00	19.35	30.3	142.5
7706-50	4902	0.78	0.3500	6.00	5.95	20.3	40.3
7610-08	2060	1.50	0.2904	10.00	9.85	25.0	37.1
MANOP H	3500	0.90	0.1130	0.66	0.65	20.3	4.7
MANOP M	3100	1.20	0.1700	1.00	0.99	14.1	8.2
MANOP C	4450	0.36	0.3820	1.80	1.79	16.0	11.3
MANOP S	4915	0.90	0.2240	1.00	0.99	3.1	11.5
P7	3085	0.97	0.6000	3.30	3.27	36.0	29.1
SO12-98	3371	0.33	0.7540	2.50	2.49	3.1	14.9
SO12229	3327	0.11	0.6140	3.20	3.20	7.6	7.6
SO26-12	3105	1.49	0.2850	1.36	1.34	10.6	15.0
SO26-58	3200	0.50	0.6940	3.20	3.18	16.0	20.8
SO26-90	2211	0.18	0.5880	3.90	3.89	20.3	8.2
SO26-96	2706	0.79	0.4570	2.05	2.04	36.0	14.7
SO26127	2463	0.11	0.5930	6.00	5.99	36.0	8.6
SO26131	3381	0.98	0.6280	3.81	3.77	30.3	35.4
SO35101	3125	0.22	0.8220	1.20	1.20	3.4	7.2
SO35102	2910	0.13	0.6230	1.28	1.27	3.4	4.3
SO35211	2890	0.09	0.2750	1.43	1.43	2.3	2.3
MD77200	2910	0.24	0.6200	3.75	3.74	4.4	12.4
MD77203	2442	2.10	0.6200	21.43	21.00	100.0	127.9
KL 5	3335	0.21	0.6800	2.00	2.00	20.3	9.1
KL 11	3859	0.37	0.8400	2.75	2.74	22.6	20.2

4. Equation (1) does not include the oxygen concentration of the deep ocean as a variable. This approach is based on the line of evidence presented by Suess [1980] and Sarnthein et al. [1987], who showed that the accumulation rate of organic carbon (C_A) is not controlled by the oxygen content of the bottom water as long as it exceeds about 100 μmol/kg. The variable oxygen concentration in the oxygen minimum layer near the oceanic thermocline may to some degree enter the equation by the exponent of z. We may assume that the F_C indeed influences the ocean chemistry and its O_2 content seasonally [Walsh et al., 1988]. However, the ocean chemistry, especially that of the ocean at more than a few centimeters above the diffusive boundary layer at the seafloor, hardly influences F_C when more than 50-100 μmol O_2/kg is available.

5. In most cases, fossil time slices and sedimentation rates were determined by identifying events in the oxygen isotope stratigraphy; only a few of the cores (mainly from the east Atlantic, east Pacific, and Indian oceans) have been C-14 dated. The end of Termination I_B has been dated at about 8000 years B.P., the onset of Termination I_A at 15,000 years B.P. The onset of stage 2 at 27,000 years B.P. (Figure 2) is different from Prell et al. [1986], the stage 2/3 boundary being placed at the top of the ~0.5‰ slope marking the base of the $\delta^{18}O$ trough of stage 2 [Duplessy et al., 1981; Vincent and Berger, 1985; Paterne et al., 1986; Bard et al., 1987; Sarnthein et al., 1982b, 1987]. Unfortunately, in many cases, the time slice "8000 years B.P. to Present" is incomplete because of the loss of the sediment surface during coring. In these cases, the interval only comprises the peak Holocene interval of 8000 to 6000/4000 years B.P. or less (Figure 2).

6. We did not systematically analyze the chemical composition of the organic carbon fraction in the sediments, which may partly originate from terrigenous organic matter and therefore may not be completely derived from marine productivity [e.g., Stein et al., 1986]. However, the stable isotopic composition of organic carbon was determined for some core profiles (Figure 5). The average $\delta^{13}C$ values of -18 to -21‰ suggest that the bulk of the carbon deposited close to a continent in zones with modern and glacial high carbon accumulation rates is derived from marine production (see below). This conclusion is corroborated by C/N values of 7-9 off northwest Africa [Hartmann et al., 1976].

7. In our calculations the long-term diagenetic loss of organic carbon was only considered for sediment sections with extremely low deposition rates of less than 0.5 cm/1000 years (applying formula (1) of Müller and Mangini [1980], for Pacific cores 10127-10175; Table 3). Occasionally, short-term losses may have also occurred due to long-term sediment storage in core repositories.

The CO_2 content of the ocean bottom water was deduced from the $\delta^{13}C$ composition of the elevated epifaunal foraminifer *Cibicidoides wuellerstorfi* [Lutze and Thiel, 1987]. As shown by Zahn et al. [1986] and postulated by Woodruff et al. [1980], Graham et al. [1981], Duplessy et al. [1984], and Berger and Vincent [1986], the carbon isotope composition of this species is fairly independent of the local carbon fluxes but depicts the general CO_2 concentration of the deep water. However, as to be expected from data of Kroopnick [1971], the data of this paper and of Zahn-Knoll [1986] reveal that regional maxima of carbon fluxes to the seafloor can also modify the general carbon isotope level of near-bottom sea-water. This influence will be reflected in the $\delta^{13}C$ content of *C. wuellerstorfi* by the same degree. Nevertheless, this factor appears to be much weaker than the pore water effect observed for the $\delta^{13}C$ values of the infaunal genus *Uvigerina* [Zahn et al., 1986; Altenbach and Sarnthein, 1988].

Fig. 2. (Opposite) (a-g) Stable isotopic records of *C. wuellerstorfi* (per mill versus PDB) and new paleoproductivity records (g m^{-2} yr^{-1}) versus time in cores used for this study (order of cores: from north to south, following Table 3). Stars represent ^{14}C dates. The $\delta^{13}C$ values were omitted where $\delta^{18}O$ values of *C. kullenbergi* replace those of *C. wuellerstorfi*. PL1, *Globigerinoides ruber*; PL2, *Neogloboquadrina pachyderma*; U. sp., *Uvigerina* sp. Further data from previously published records and from personal unpublished communications (1987) in Table 3. The onset age of Termination IA is shown by dotted line normally based on benthic $\delta^{18}O$ record. "C-14" marks onset ages derived from radiocarbon dates (stars); "P" marks onset ages obtained from planktonic $\delta^{18}O$ curves (not shown because of format problems) where *C. wuellerstorfi* values were incomplete or based on too small specimen numbers.

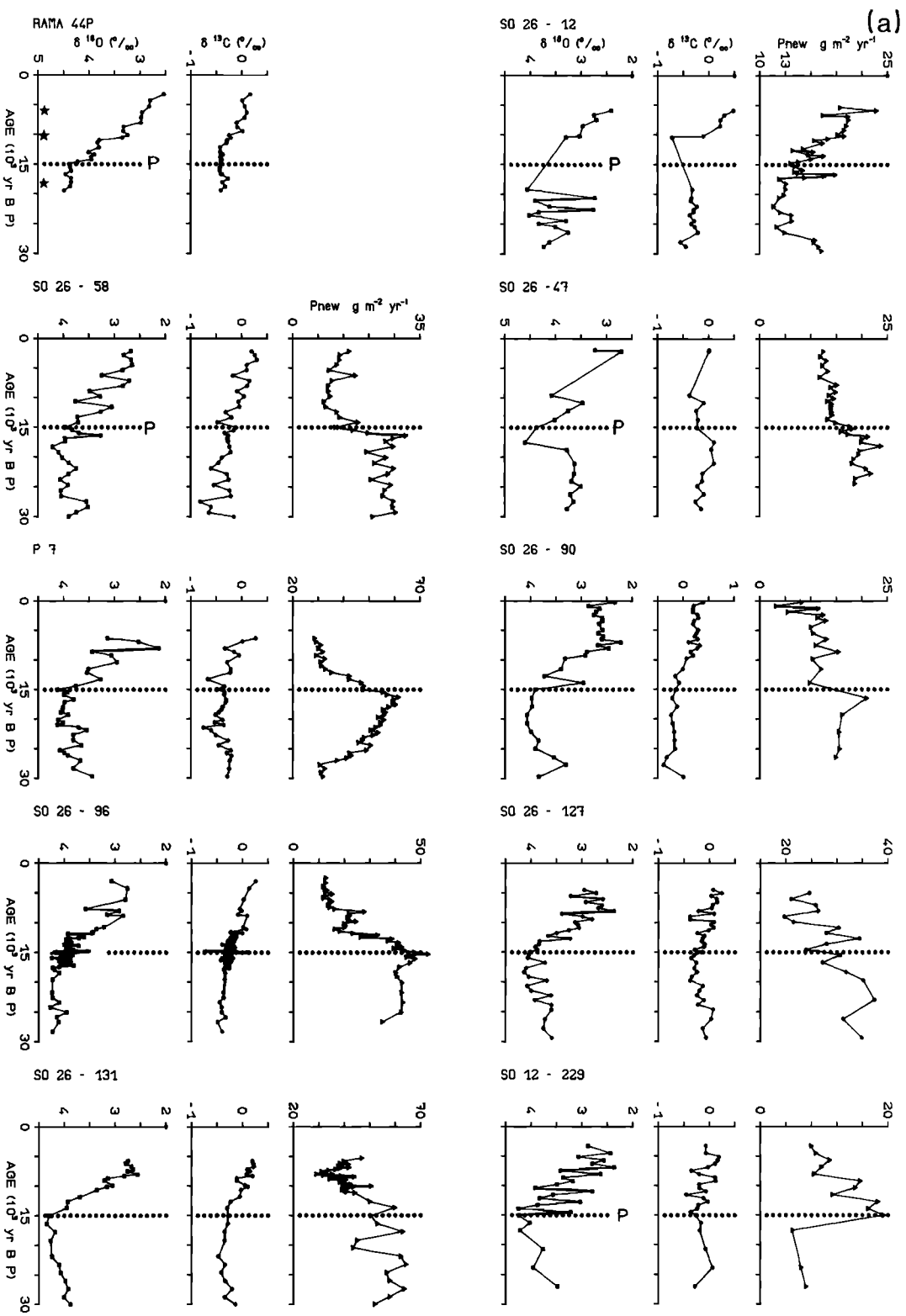
(a)
RAMA 44P
SO 26 - 12
SO 26 - 47
SO 26 - 58
SO 26 - 90
P 7
SO 26 - 96
SO 26 - 127
SO 26 - 131
SO 12 - 229
δ 18O (‰)
δ 13C (‰)
Pnew g m-2 yr-1
AGE (10³ yr B P)
P

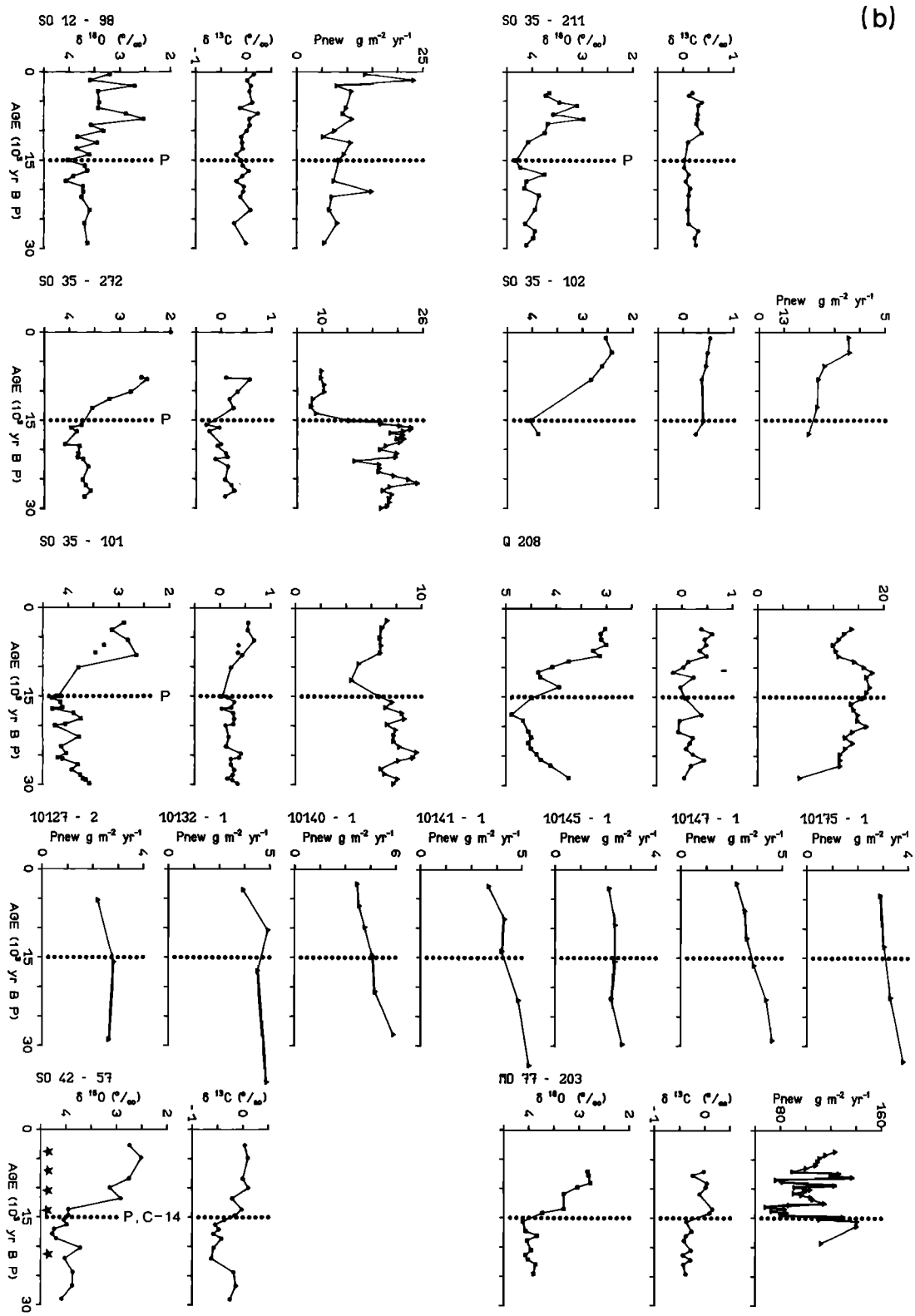

Fig. 2. (continued)

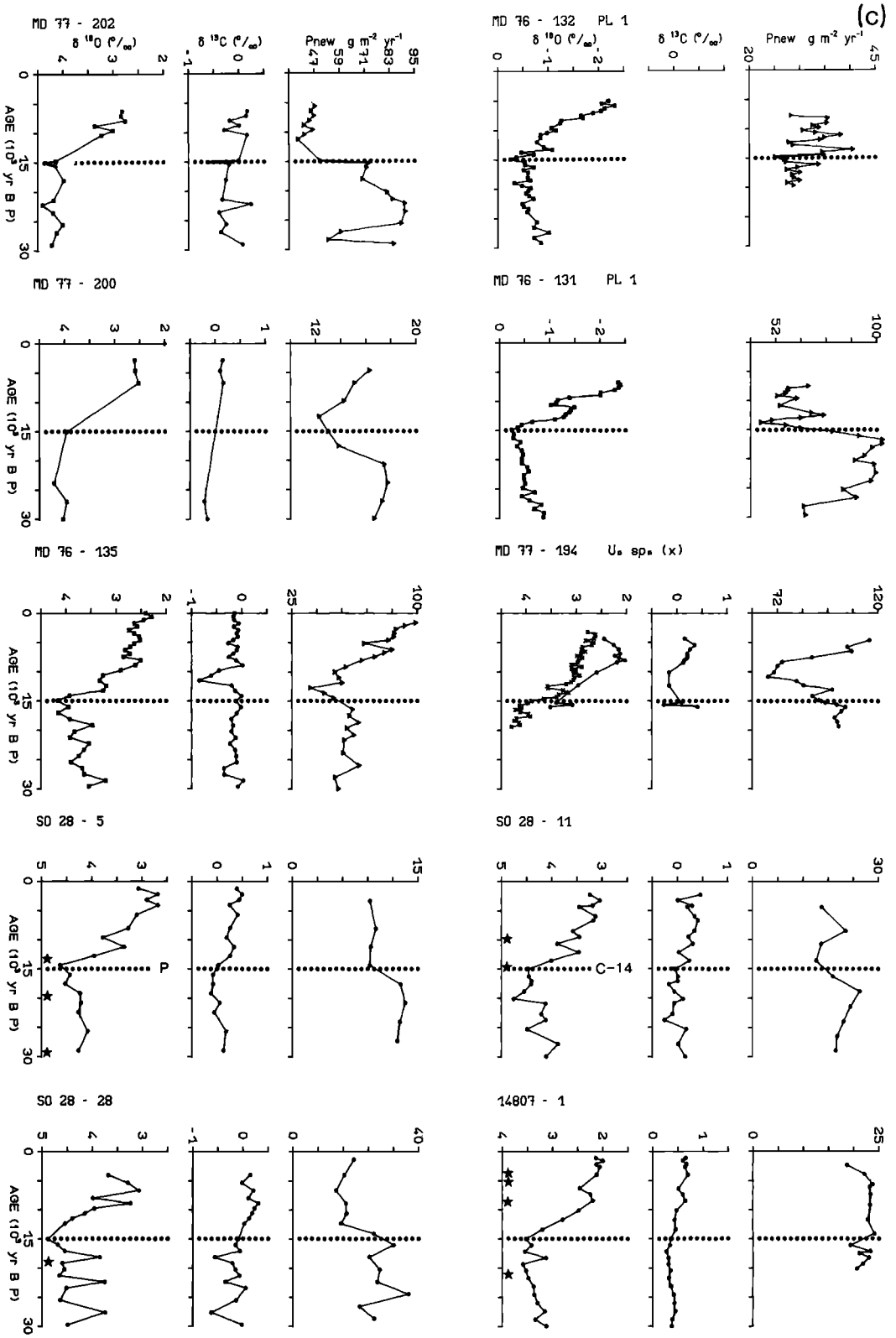

Fig. 2. (continued)

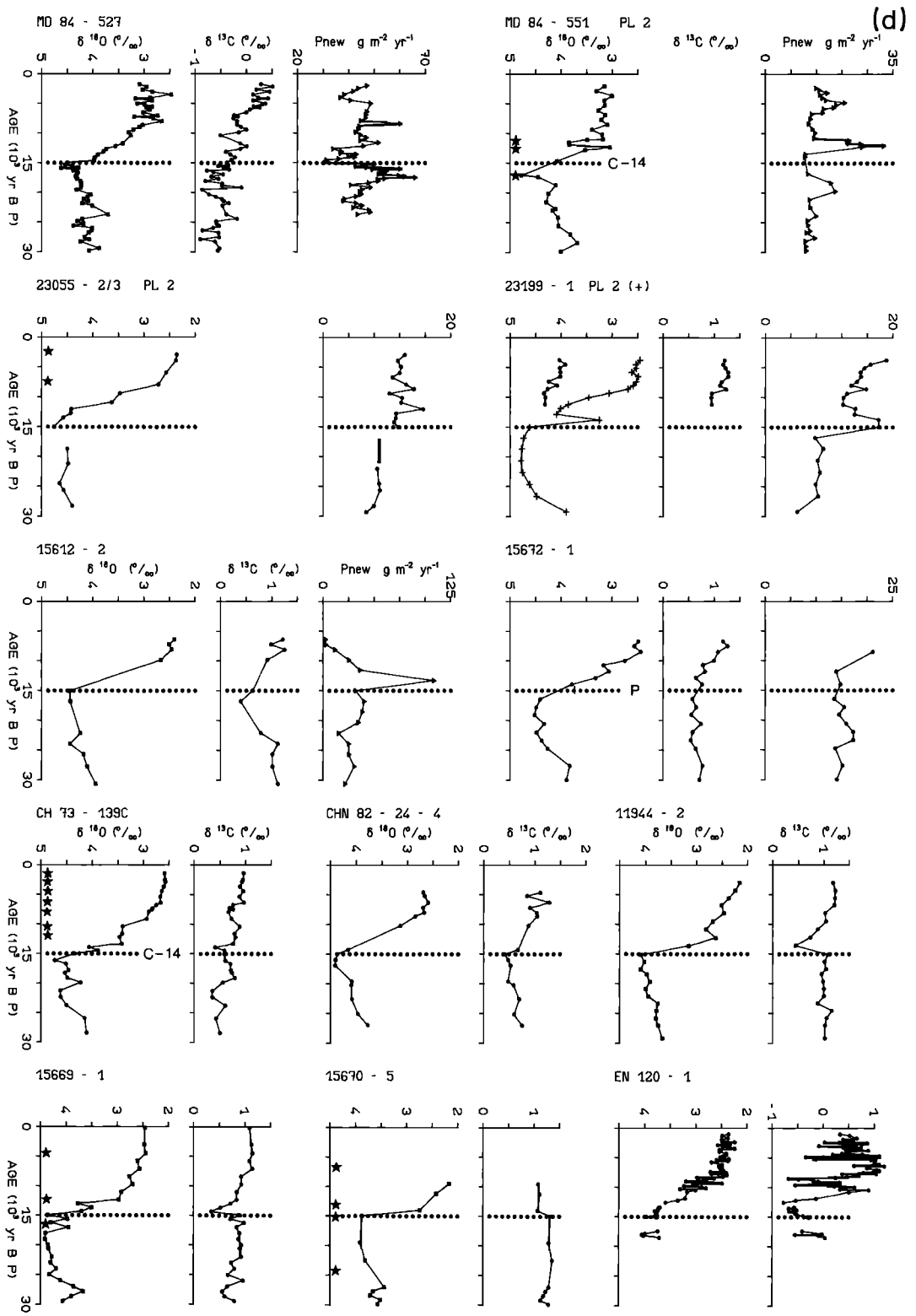

Fig. 2. (continued)

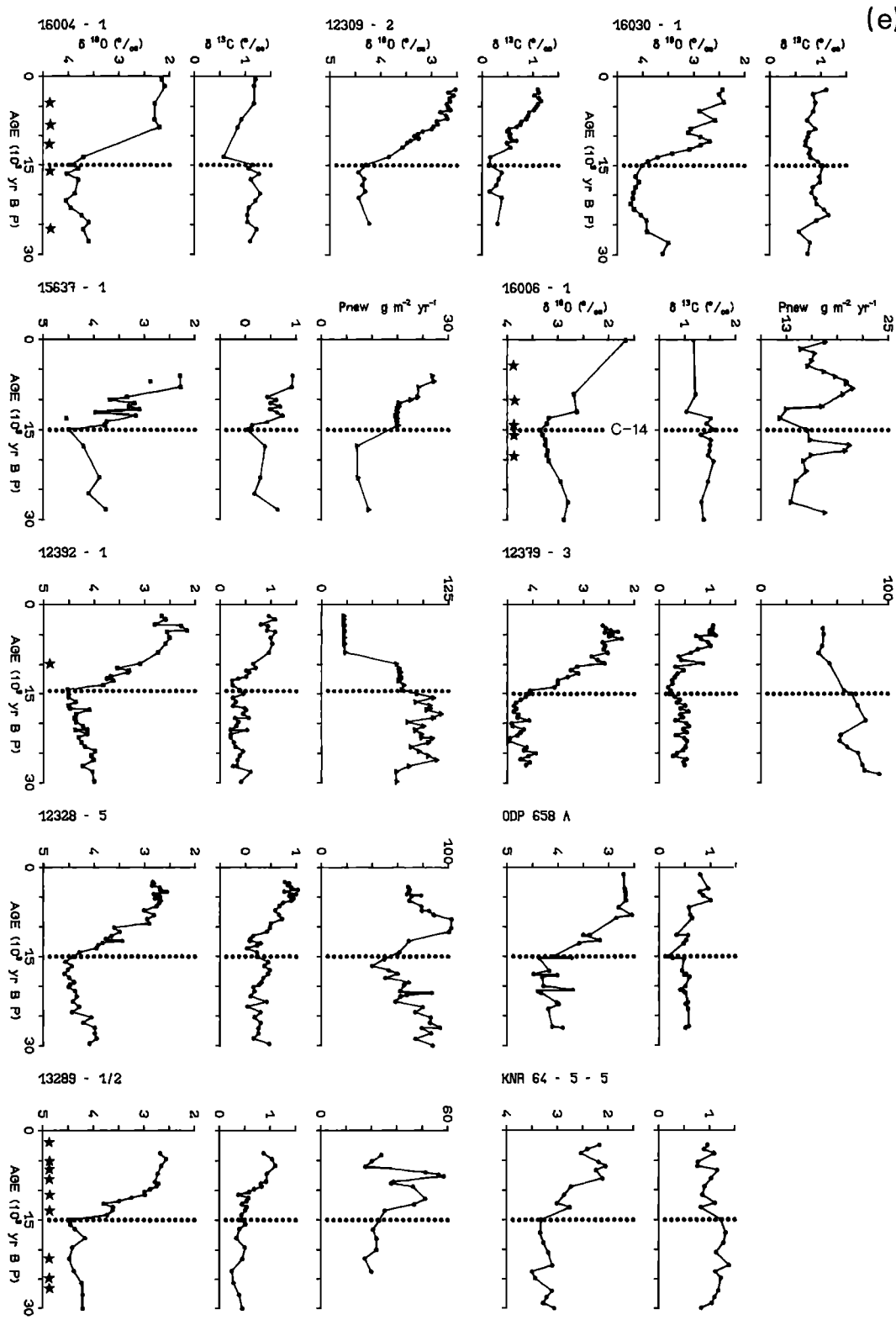

Fig. 2. (continued)

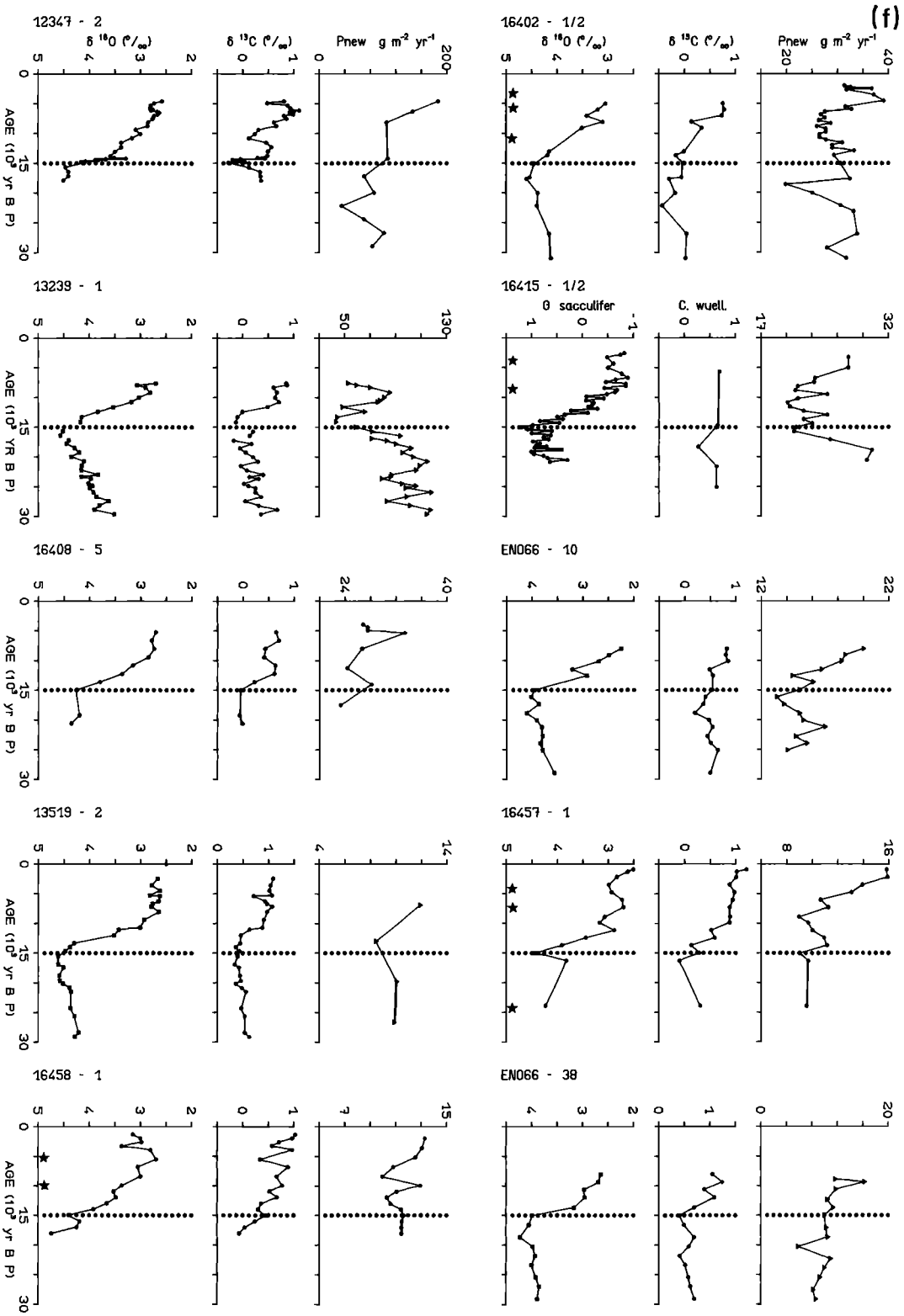

Fig. 2. (continued)

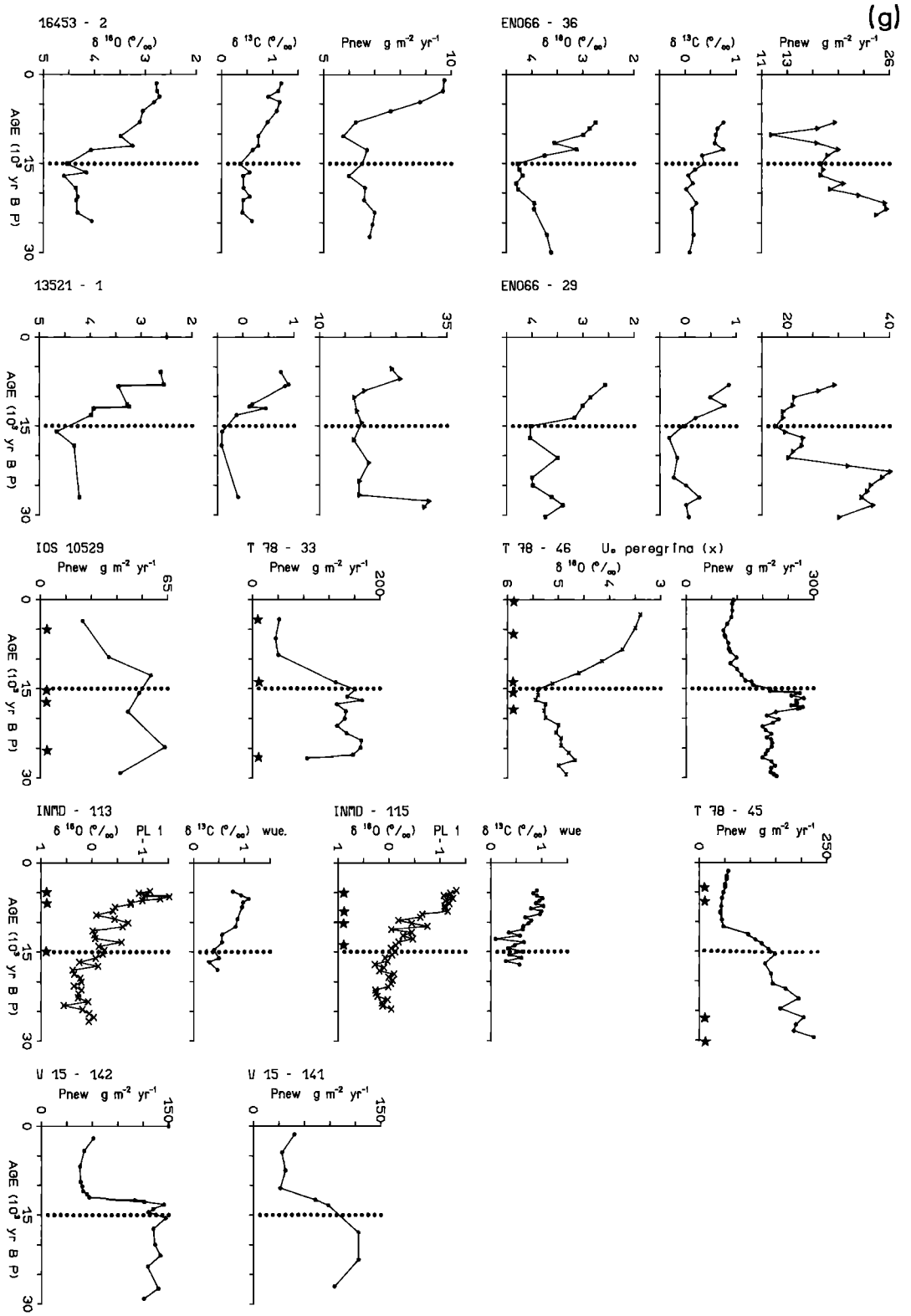

Fig. 2. (continued)

TABLE 3. Core Locations, Water Depths, Average $\delta^{13}C$ Values and New Paleoproductivity Data From the LGM (17,000-21,000 Years B.P. and the Holocene (Last 8000 Years) Used in This Paper

Core Number	Latitude	Longitude	Depth, m	$\delta^{13}C$ ‰ 0-8k	$\delta^{13}C$ ‰ 17-21k	$\Delta\delta^{13}C$	Production, g/m²yr 0-8k	Production, g/m²yr 17-21k	Production, g/m²yr ΔPnew %	Reference
					Pacific Ocean					
ARAMA 44P	53°00.0'N	164°39.2'W	2980	0.05	-0.35	0.40	-	-	-	c10
*Y69-10-2	41°16.0'N	126°24.0'W	2743	0.01	-0.57	0.58	-	-	-	c3
*V32-128	36°28.0'N	177°10.0'E	3623	0.31	-0.17	0.48	-	-	-	c3
*SO50-37	18°54.6'N	115°45.8'W	2695	0.16	-0.25	0.41	-	-	-	a
*SO50-29	18°26.1'N	115°39.2'W	3766	0.22	-0.20	0.42	-	-	-	a
ASO26-12	13°07.3'N	103°00.5'W	3105	0.33	-0.34	0.67	20.2	13.1	54.2	a
*RC13-120	3°51.0'N	107°14.0'W	3753	0.10	-0.40	0.50	-	-	-	c3
*V17-42	3°32.0'N	81°11.0'W	1814	0.01	-0.24	0.25	-	-	-	c3
ASO26-58	2°43.7'N	95°11.3'W	3200	0.19	-0.32	0.51	12.6	24.2	-48.0	a
ASO26-47	2°39.8'N	100°15.0'W	4027	-	-	-	12.8	20.1	-36.0	a
AP 7	2°36.3'N	83°59.2'W	3085	0.14	-0.42	0.56	29.6	56.2	-47.4	a,c1
ASO26-90	2°15.0'N	92°20.9'W	2211	0.25	-0.19	0.43	9.9	16.1	-38.6	a
*W8402A-14	0°57.2'N	138°57.3'W	4287	-	-	-	9.7	12.8	-24.1	c12
ASO26-96	0°41.1'N	85°50.4'W	2706	0.10	-0.32	0.42	13.4	41.2	-67.4	a
*V24-109	0°26.0'N	158°48.0'E	2367	0.31	0.11	0.20	-	-	-	c3
*KN73-3	0°22.0'S	106°11.0'W	3606	0.22	-0.22	0.44	-	-	-	c4
*V19-27	0°28.0'S	82°04.0'W	1373	0.32	-0.03	0.35	-	-	-	c3
ASO26-127	1°32.8'S	85°23.1'W	2463	0.06	-0.28	0.34	24.0	33.5	-28.5	a
*V19-28	2°28.0'S	84°39.0'W	2670	-	-	-	29.9	60.4	-50.5	c12
*V19-30	3°23.0'S	83°21.0'W	3091	0.03	-0.43	0.46	-	-	-	c3
ASO26-131	3°31.6'S	85°00.2'W	3381	0.16	-0.35	0.51	37.3	50.4	-26.0	a
*TR16-331	3°58.0'S	83°52.0'W	3209	0.02	-0.34	0.36	-	-	-	c3
ASO12-229	4°14.4'S	103°54.3'W	3327	-0.03	-0.14	0.11	9.1	5.1	80.0	a
BSO12-98	10°32.1'S	109°44.7'W	3371	0.07	-0.10	0.17	12.1	11.0	10.1	a
BSO35-211	14°23.2'S	177°08.7'E	2890	0.26	0.10	0.15	?2.7	3.0	-11.5	a
BSO35-272	16°01.2'S	177°41.4'E	3410	0.37	0.00	0.37	9.8	21.5	-54.3	a
BSO35-102	22°24.3'S	177°26.9'W	2910	0.45	?0.24	?0.21	3.0	2.0	54.0	a
BSO35-101	22°26.9'S	177°19.8'W	3125	0.56	0.20	0.36	6.8	8.1	-15.2	a
BQ208	45°59.2'S	177°59.3'W	2830	0.46	0.09	0.37	13.1	15.8	-17.5	a
B10127-2	13°41.7'N	151°39.3'W	5686	-	-	-	2.2	2.8	-22.2	a10
B10132-1	6°13.2'N	148°57.3'W	5004	-	-	-	3.7	4.4	-16.4	a10
B10140-1	9°15.0'N	148°44.5'W	5144	-	-	-	3.7	4.8	-21.7	a10
B10141-1	9° 6.2'N	148°46.7'W	5189	-	-	-	3.3	4.8	-31.2	a10
B10145-1	3°59.5'N	148°49.3'W	4599	-	-	-	2.1	2.5	-13.0	a10
B10147-1	3°50.2'N	145° 1.7'W	4619	-	-	-	3.0	3.9	-24.7	a10
B10175-1	9°19.3'N	146° 1.1'W	5164	-	-	-	2.9	3.3	-13.0	a10
					Indian Ocean					
BSO42-57	20°54.5'N	63°07.3'E	3422	0.07	-0.50	0.57	-	-	-	a,a1
BMD77-203	20°41.2'N	59°34.0'E	2442	-0.13	-0.33	0.20	111.4	112.0	- 0.5	b,a
CMD77-202	19°13.0'N	60°40.2'E	2427	0.05	-0.26	0.31	46.1	75.8	-39.2	b,a

TABLE 3. (continued)

Core Number	Latitude	Longitude	Depth, m	$\delta^{13}C$ ‰ 0-8k	$\delta^{13}C$ ‰ 17-21k	$\Delta\delta^{13}C$	Production, g/m²yr 0-8k	Production, g/m²yr 17-21k	ΔPnew %	Reference
				Indian Ocean						
CMD76-132	16°59.0'N	71°30.1'E	1430	-	-	-	28.0	28.7	- 1.8	b,a
CMD77-200	16°32.1'N	67°53.1'E	2910	0.14	-	-	15.7	15.6	0.6	b,a
CMD76-131	15°31.1'N	72°34.0'E	1230	-	-	-	62.6	96.6	-35.2	b,a
CMD76-135	14°26.0'N	50°31.1'E	1895	-0.14	-0.17	-0.03	82.4	60.9	35.3	b,a
*MD76-128	13°08.0'N	73°19.0'E	1712	0.09	-0.13	0.22	-	-	-	b
*MD76-127	12°05.0'N	75°54.0'E	1610	0.21	-0.37	0.58	-	-	-	b
CMD77-194	10°28.0'N	75°14.0'E	1222	0.22	-	-	104.3	100.3	4.0	b
*MD76-125	8°35.0'N	75°20.0'E	1878	0.23	-0.08	0.31	-	-	-	b
CSO28-5	6°39.8'N	61°08.0'E	3335	0.38	-0.05	0.43	9.6	13.3	-27.5	a,a2
CSO28-11	5°23.4'N	60°15.1'E	3859	0.28	-0.03	0.31	16.5	24.4	-32.4	a,a2
CSO28-28	1°24.3'N	67°21.9'E	4101	0.11	-0.25	0.36	16.5	25.9	-36.4	a,a2
*V34-55	6°02.4'S	88°57.4'E	2992	-	-	0.20	-	-	-	c2
*V34-54	6°05.0'S	89°10.0'E	3254	-	-	0.40	-	-	-	c2
*V34-51	6°11.5'S	89°58.0'E	4382	-	-	0.60	-	-	-	c2
C14807-1	16°56.2'S	118°50.5'E	1186	0.62	0.31	0.31	22.2	22.0	1.0	a,a3
*MD79-254	17°53.0'S	38°40.0'E	1934	0.65	0.03	0.62	-	-	-	b
				Southern Ocean						
*RC11-120	43°31.0'S	79°52.0'E	3135	0.46	-0.37	0.83	-	-	-	c3
DMD84-527	43°49.3'S	51°19.1'E	3262	0.15	-0.58	0.73	43.8	50.7	-13.6	b
DMD84-551	55°00.5'S	73°16.9'E	2230	-	-	-	16.1	18.6	-13.4	b1
				Atlantic Ocean						
D23055-2	68°24.4'N	4°01.3'E	2308	1.32	-	-	12.1	8.8	37.5	a4
D23199-1	68°22.6'N	5°13.5'E	1968	1.20	-	-	15.5	8.6	80.3	a5
*V28-14	64°47.0'N	29°34.0'W	1855	0.62	1.41	-0.79	-	-	-	c3
*DSDP552	56°03.0'N	23°13.0'W	2311	1.29	0.94	0.35	-	-	-	c3
DCH73-139C	54°38.0'N	16°21.0'W	2209	0.86	0.71	0.15	-	-	-	b
*NO75-08	45°42.0'N	31°22.0'W	3454	1.07	0.59	0.48	-	-	-	b
D15612-2	44°41.6'N	26°32.6'W	3050	1.10	0.55	0.55	2.4	36.5	-93.4	a,a3
*V29-179	44°00.0'N	24°32.0'W	3331	1.10	0.63	0.47	-	-	-	c3
*CH82-5020	43°29.9'N	29°52.0'W	3020	1.25	0.60	0.65	-	-	-	c4
*S58798	42°50.0'N	23°04.0'W	3520	0.92	0.60	0.32	-	-	-	c3
DCH82-24-4	41°43.0'N	32°51.0'W	3427	1.04	0.53	0.51	-	-	-	c4
*CH72-02	40°36.0'N	21°42.0'W	3485	0.91	0.77	0.14	-	-	-	b
*CH74-23-1	36°52.0'N	26°37.0'W	2354	1.00	0.56	0.44	-	-	-	b
D11944-2	35°39.1'N	8° 3.7'W	1765	1.21	1.00	0.21	-	-	-	a3
D15670-5	34°54.5'N	7°34.6'W	1482	?1.08	1.29	-0.20	-	-	-	a3
D15669-1	34°53.5'N	7°48.9'W	2022	1.15	0.90	0.25	-	-	-	a3
D15672-1	34°51.6'N	8°07.6'W	2455	1.22	0.65	0.57	-	15.3	-	a,a3
DEN120-1	33°40.0'N	57°37.0'W	4450	0.60	-0.20	0.80	-	-	-	c4
E16004-1	29°58.7'N	10°38.8'W	1512	1.12	1.20	-0.08	-	-	-	a3
E16006-1	29°14.8'N	11°29.8'W	796	1.17	1.50	-0.33	17.3	17.8	- 2.4	a,a3

TABLE 3. (continued)

Core Number	Latitude	Longitude	Depth, m	$\delta^{13}C$ ‰ 0-8k	$\delta^{13}C$ ‰ 17-21k	$\Delta\delta^{13}C$	Production, g/m²yr 0-8k	Production, g/m²yr 17-21k	ΔPnew %	Reference
				Atlantic Ocean						
E15637-1	27°00.3'N	18°59.2'W	3849	0.92	0.38	0.54	25.2	8.4	200.0	a
E12309-2	26°50.3'N	15°06.6'W	2820	0.99	0.29	0.70	-	-	-	a3
E12392-1	25°10.3'N	16°50.7'W	2575	0.97	0.40	0.57	22.3	105.0	-78.8	a,a6,c3
E12379-3	23°08.1'N	17°44.7'W	2576	0.93	0.47	0.46	47.9	79.3	-39.6	a,a3,a7
*V23-100	21°18.0'N	22°41.0'W	4579	0.59	0.00	0.59	-	-	-	c5
E16030-1	21°14.1'N	18°03.3'W	1500	0.88	0.89	-0.01	-	-	-	a3
E12328-5	21°08.7'N	18°34.4'W	2778	0.82	0.31	0.51	73.5	60.0	22.6	a,a3
EODP658A	20°45.0'N	18°34.9'W	2263	0.80	0.49	0.31	-	-	-	a8
E13289-2	18°04.4'N	18°00.6'W	2490	0.98	0.42	0.56	38.5	26.3	50.0	a,a3,a7
EKNR64-5-5	16°31.3'N	74°48.4'W	3047	0.95	1.25	0.30	-	-	-	c4
F12347-2	15°49.5'N	17°51.7'W	2576	0.88	0.35	0.53	166.7	78.2	113.0	a3,a7
F16402-2	14°27.5'N	20°32.5'W	4234	0.60	-0.18	0.78	31.8	25.8	23.1	a
*V22-197	14°10.0'N	18°35.0'W	3167	0.76	0.17	0.59	-	-	-	c3
F13239-1	13°52.6'N	18°18.8'W	3156	0.86	0.08	0.78	55.9	98.0	-43.0	a
*V22-196	13°50.0'N	18°58.0'W	3728	0.85	-0.20	1.05	-	-	-	c3
*CH75-03	10°03.0'N	57°32.0'W	3410	0.84	0.13	0.71	-	-	-	b
*CH75-04	10°01.0'N	56°01.0'W	3820	0.94	-0.21	1.15	-	-	-	b
F16415-1/2	9°34.0'N	19°06.4'W	3841	0.69	0.27	0.42	25.0	29.8	-15.0	a,a4
F16408-5	9°00.3'N	21°21.9'W	4336	0.59	-0.04	0.63	28.4	23.3	21.9	a,a4
FENO66-10	6°20.0'N	21°53.9'W	3527	0.82	0.34	0.48	20.0	14.7	36.0	c6
F13519-2	5°39.5'N	19°51.0'W	2862	0.99	0.43	0.56	11.9	10.1	18.0	a,a9
*ENO66-16	5°27.3'N	21° 8.6'W	3152	0.97	0.43	0.54	-	-	-	c6
F16457-1	5°23.5'N	21°43.2'W	3291	1.00	0.11	0.89	13.4	9.6	39.7	a,a4
F16458-2	5°20.1'N	22° 3.4'W	3518	0.80	-0.02	0.82	12.1	11.5	5.7	a,a4
*ENO66-44	5°15.8'N	21°42.7'W	3428	1.05	0.50	0.55	-	-	-	c6
FENO66-38	4°55.2'N	20°30.0'W	2931	1.05	0.64	0.41	-	8.9	-	c6
G16453-2	4°44.1'N	20°56.8'W	2675	1.01	0.47	0.54	8.4	6.3	33.3	a,a4
*CH71-07	4°23.0'N	20°52.0'W	3083	1.08	0.30	0.78	-	-	-	b
GENO66-36	4°18.4'N	20°12.7'W	4270	0.75	0.08	0.67	19.5	20.0	- 2.5	c6
*ENO66-21	4°14.0'N	20°37.3'W	3995	0.84	0.12	0.72	-	-	-	c6
*ENO66-26	3°05.1'N	20°01.0'W	4745	0.68	-0.20	0.88	-	-	-	c6
G13521-1	3°01.2'N	22°01.9'W	4504	0.82	-0.42	1.24	25.0	18.2	37.0	a,a7
*ENO66-32	2°28.4'N	19°44.1'W	5003	0.89	-0.12	1.01	-	-	-	c6
GENO66-29	2°27.6'N	19°45.7'W	5104	0.85	-0.24	1.09	29.2	21.7	34.0	c6
*V25-59	1°22.0'N	33°29.0'W	3824	0.89	0.07	0.82	-	-	-	c5
GIOS-10529	4°56.8'S	0°27.7'E	4735	-	-	-	21.5	44.6	-51.8	c7
GT78- 33	5°11.0'S	7°58.0'E	4120	-	-	-	38.7	148.5	-74.0	c11
GT78- 46	6°50.1'S	10°45.3'E	2100	-	-	-	100.9	239.0	-57.8	c11
GT78- 45	7°47.8'S	10°07.0'E	4070	-	-	-	49.7	137.7	-63.9	c11
*V22-174	10°04.0'S	12°49.0'W	2630	0.80	0.72	0.08	-	-	-	c3
GINMD-113	15°15.0'S	14°58.0'W	3471	0.94	0.47	0.47	-	-	-	c8
GINMD-115	17°40.0'S	16°13.0'W	3427	0.92	0.48	0.44	-	-	-	c8
*RC13-228	20°20.0'S	11°12.0'E	3204	0.50	-0.10	0.60	-	-	-	c3

TABLE 3. (continued)

Core Number	Latitude	Longitude	Depth, m	δ13C ‰ 0-8k	δ13C ‰ 17-21k	Δδ13C	Production, g/m2yr 0-8k	Production, g/m2yr 17-21k	ΔPnew %	Reference
				Atlantic Ocean						
*CHN115-70	29°55.2'S	35°39.3'W	2340	0.95	0.71	0.24	-	-	-	c6
*CHN115-91	30°49.5'S	38°25.8'W	3576	0.62	0.23	0.39	-	-	-	c6
*CHN115-92	30°50.3'S	38°50.5'W	3934	0.13	-0.43	0.56	-	-	-	c6
*CHN115-88	30°55.0'S	36°04.8'W	2941	0.68	0.34	0.34	-	-	-	c6
*AII60-13A	31°59.1'S	36°38.9'W	2739	1.17	0.43	0.71	-	-	-	c6
*RC12-294	37°16.0'S	10°06.0'W	3308	0.81	-0.23	1.04	-	-	-	c3
GV15-142	44°54.0'S	51°32.0'W	5885	-	-	-	52.3	132.7	-60.6	c9
GV15-141	45°44.0'S	50°45.0'W	5934	-	-	-	39.8	123.6	-67.8	c9

References: a, this work (Kiel); a1, Kiel (F. Sirocko, unpublished, 1988); a2, Heidelberg [Scholten, 1987]; a3, Kiel [Zahn-Knoll, 1986]; a4, Kiel (E. Vogelsang and H. Kassens, unpublished, 1987); a5, Kiel (R. Zahn-Knoll, unpublished, 1986; Ramm, [1986]); a6, Kiel/Oregon [Thiede et. al., 1982]; a7, Kiel [Hartmann et al., 1976]; a8, Kiel (R. Tiedemann, unpublished, 1988); a9, Kiel [Müller et al., 1983]; a10, Kiel/Heidelberg [Müller and Mangini, 1980; Cochran, 1985]; b, this work (Gif-sur-Yvette); b1, Gif-sur-Yvette [Pichon et al., 1987]; c1, Vancouver [Pedersen et al., 1988]; c2, Brown [Peterson, 1985]; c3, Cambridge [N. J. Shackleton, various sources, to 1987]; c4, Cambridge Mass. [Boyle and Keigwin, 1985, 1987]; c5, Lamont (R. G. Fairbanks, unpublished, 1987); c6, Woods Hole [Curry and Lohmann, 1984]; c7, Wormley [Morris et al., 1984]; c8, Scripps [Vincent and Berger, 1986]; c9, [Stevenson and Cheng, 1972]; c10, Woods Hole [Keigwin, 1987]; c11, Texel [Jansen et al., 1984; and unpublished data, 1987; Olausson, 1984]; c12, Lyle et al., 1988].

The 13C averages exclude values obviously affected by bioturbation. Data sources listed at end of table (above). Asterisks represent data not depicted in Figure 2. The prefix A-G on core numbers refers to Figures 2a-2g.

Most oxygen and carbon isotope data provided by the Kiel group were measured according to standard procedures [Duplessy, 1978; Ganssen, 1983] on a Finnigan MAT 251 mass spectrometer combined with a new, fully automated carbonate preparation line (CARBO-KIEL; C-14 Laboratory, Christian-Albrechts-Universität, Kiel, Dr. H. Erlenkeuser, and Finnigan Bremen, Dr. K. Habfast; for details see Zahn et al. [1986]). The stable isotope data provided by the Centre des Faibles Radioactivites, Gif-sur-Yvette, were analyzed on a VG 602D micromass spectrometer. The unpublished isotope values kindly provided by Peterson [1985] were measured at a Sira 903 at Brown University, Providence, Rhode Island (compare Table 3). The oxygen isotopic stratigraphy of many sediment cores from the Indian and Pacific oceans was corroborated by additional planktonic $\delta^{18}O$ records.

RESULTS

The $\delta^{13}C$ Record of Global Shifts in the Concentration of Oceanic Bottom Water CO_2 During Termination I

From about 105 $\delta^{18}O$/ $\delta^{13}C$ curves of *C. wuellerstorfi* (most of them depicted in Figure 2) two time slices were selected, which lie at 17,000-21,000 years B.P. (Last Glacial Maximum, LGM) and 0-8000 years B.P. (Holocene), and their respective $\delta^{13}C$ values averaged. By these means we expect to exclude short-term local anomalies in the deep water CO_2 concentration. The carbon isotopic difference (‰ $\Delta\ \delta^{13}C$) between the LGM and the Holocene and the source of data are presented in Table 3. The geographic distribution of

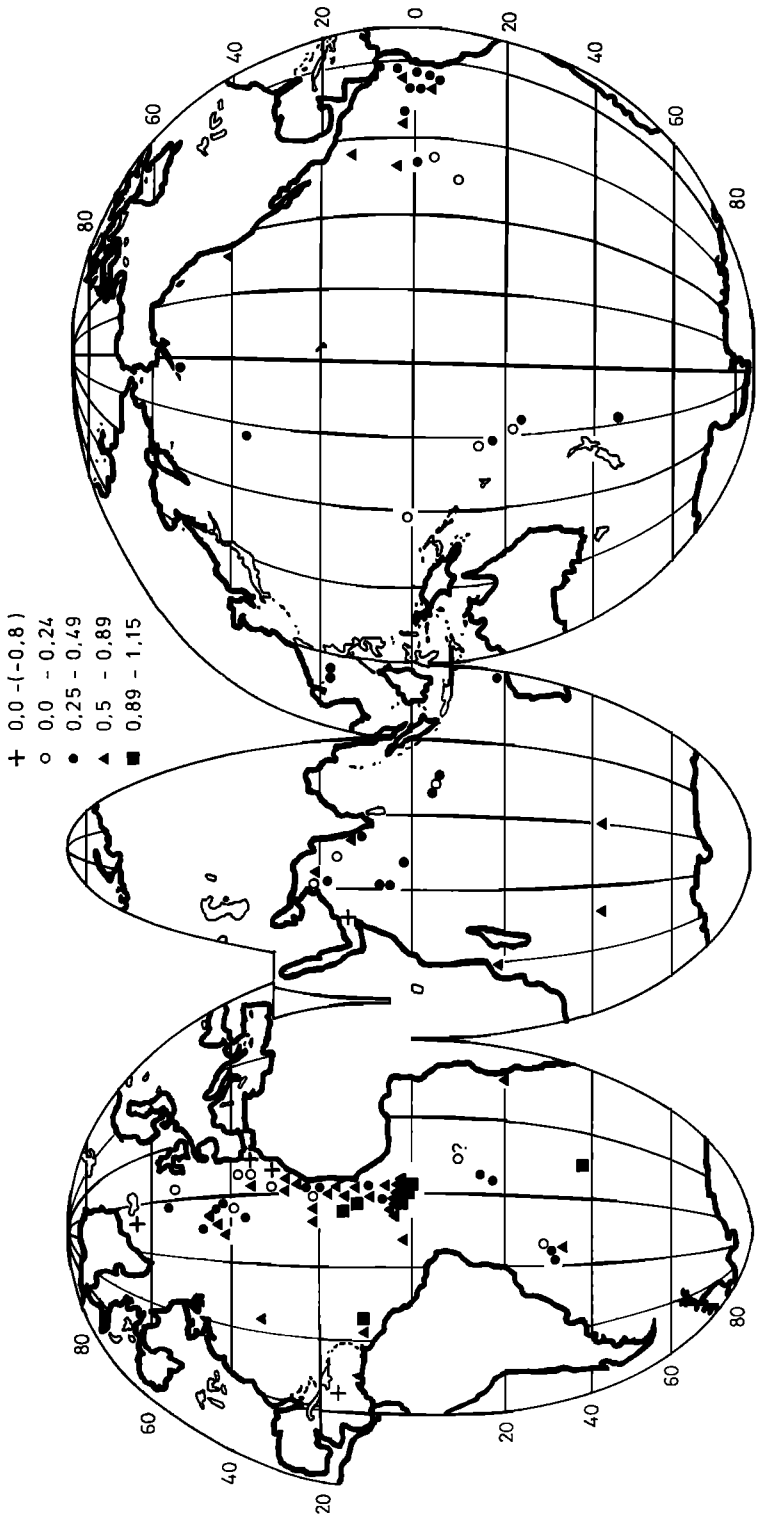

Fig. 3. Geographic distribution of δ13C differences between Last Glacial Maximum (17,000-21,000 years B.P.) and Holocene (last 8000 years). Data sources listed in Table 3. Positive values (plus signs) come from water depths between 1400 and 2000 m, except for Caribbean Sea datum.

the difference values is plotted in Figure 3. The deep water $\delta^{13}C$ level has increased by about 0.15-0.9‰ on a global scale during glacial Termination I. This difference only applies to the depth range of NADW and deeper because most sediment cores under investigation were obtained from water depths of 2000-4000 m. A regional close-up reveals some fairly systematic variations in the $\Delta\delta^{13}C$ distribution pattern. In large parts of the Pacific and northern Indian oceans the difference values lie between (0.15-) 0.2 and 0.5‰. This range may provide an idea of the changes in the carbon budget in the deep sea on a global scale as discussed below. On the other hand, most values from the Atlantic and the southern Indian oceans are somewhat higher, varying between 0.4 and 0.9‰.

Furthermore, Figure 3 (see plus signs) reveals three regions where at intermediate water depths (1000-2000 m) the $\delta^{13}C$ values did not increase but decreased from peak glacial to Holocene times. The most important area with a $\delta^{13}C$ reduction of -0.79‰ during Termination I lies southeast of Greenland at 60°N at 1855 m depth. Taking into account the local sharp $\delta^{13}C$ rise within the last 8000 years from 0.25 to 0.91‰ at the sediment surface and to 1.1‰ in a neighboring GEOSECS profile, the negative LGM-to-Holocene $\delta^{13}C$ difference is lowered to 0.5 and 0.3‰, respectively but still remains significant. The signal of ^{13}C rich deep water during glacial times can be traced further downslope to the southeast by means of unusually low positive $\Delta\delta^{13}C$ numbers (0.14-0.35‰) through the deeper northeast Atlantic basins near Rockall Bank, up to 40°N, i.e., east of the Azores at about 3500 m water depth. Most probably, this anomaly in the northern Atlantic marks the main area of NADW formation and advection during the LGM [Duplessy et al., this issue; J. Sündermann et al., Atlantic circulation during the Last Glacial Maximum--A dynamic model, submitted to *Paleoceanography*, 1988 (hereinafter referred to as JS (1988))].

A second region where $\delta^{13}C$ values have decreased by up to 0.3‰ from glacial to interglacial time, the area where the present (and past) Mediterranean Outflow Water (MOW) impinges upon the northwest African continental slope at 800-1700 m water depth, north of 22°N [Zahn-Knoll, 1986; Zahn et al., 1987]. This distribution pattern demonstrates that the outflow of Mediterranean Water was less CO_2 enriched during peak glacial times and had a stronger influence on the northeast Atlantic hydrography than today. It can be traced further south up to the equator by means of low carbon isotopic differences ranging near zero per mill along the depth range of 1000-1300 m [Zahn-Knoll, 1986]. A third small region with a slightly positive $\Delta\delta^{13}C$ anomaly (-0.03‰) lies in the outer Gulf of Aden, also at intermediate water depths of about 1900 m. This $\delta^{13}C$ decrease may be linked to an increase in local primary production and carbon flux to the seafloor since the LGM (Figure 4) as first reported by Prell and Curry [1980]. The large increases in $\delta^{13}C$ are generally restricted to cores from the deep basins of the eastern equatorial south Atlantic, mostly below 3750 m (Figure 2). In this region the $\delta^{13}C$ values of *C. wuellerstorfi* increased by more than +0.9-1.0‰ and below 5000 m water depth, even by 1.2‰ since the LGM. These high differences are caused by extremely low glacial $\delta^{13}C$ values. In part, they may be the result of advection of ^{13}C depleted Antarctic Bottom Water into the basins of the eastern south Atlantic [Curry and Lohmann, 1984]. Furthermore, we assume that enhanced fluxes of particulate carbon from local centers of high productivity in this equatorial region have added to this extreme glacial $\delta^{13}C$ minimum (see below). However, in the southeastern Atlantic, bottom conditions never became completely anaerobic, as the benthic form *C. wuellerstorfi* is continuously present through this interval of the cores. This may also occur to core IOS-10529 (Table 3) where siliceous, carbonate-free sapropels indicate anoxic conditions in the southern Bay of Guinea at 4735 m water depth, between 19,000 and 14,000 years B.P. [Morris et al., 1984]. This oxygen-depleted regime in the eastern equatorial and south Atlantic basins is clearly distinguished from the general CO_2 enrichment in the deep ocean during the LGM by the fact that it ended about 3000-5000 years earlier than the general CO_2 depletion in the deep ocean during early Termination I (Figure 6).

Below regions with a marked glacial to interglacial productivity reduction of the surface ocean (Figure 4) the average glacial to interglacial differences in $\delta^{13}C$ increase from about 0.2 to 0.5‰ to 0.4 to 0.8‰ in the open ocean. Such values occur below the divergence zone in the

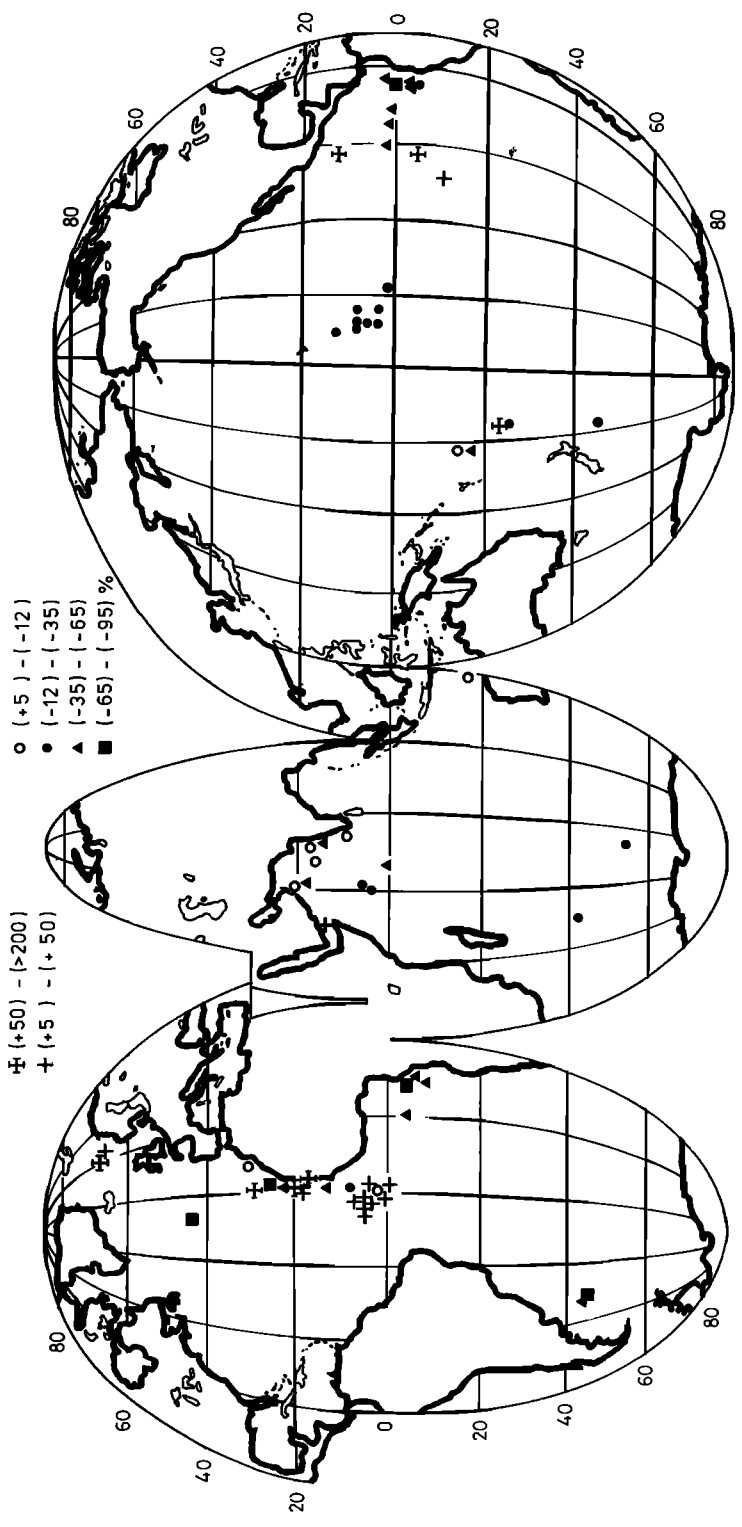

Fig. 4a. Geographic distribution of changes in new paleoproductivity from the Last Glacial Maximum (17,000-21,000 years B.P.) to the Holocene (last 8000 years). Relative changes in percent of glacial value.

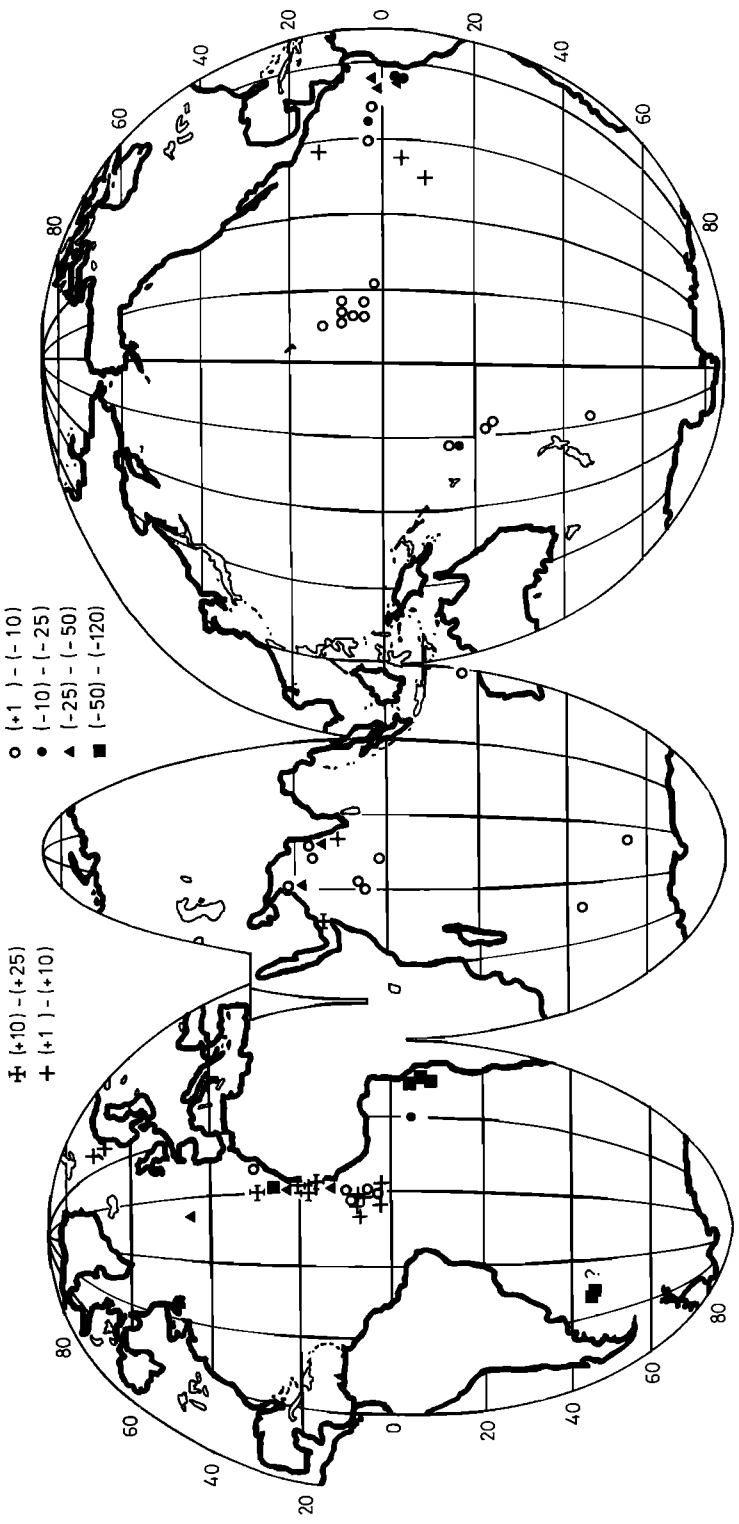

Fig. 4b. Geographic distribution of changes in new paleoproductivity from the Last Glacial Maximum (17,000-21,000 years B.P.) to the Holocene (last 8000 years). Absolute numbers (g m^{-2} yr^{-1}). Data sources listed in Table 3.

eastern equatorial Pacific, below the coastal upwelling region off Oregon, in the circum-Antarctic ocean, near coastal upwelling cells along the east Atlantic continental margin, and in a few cores from the Mid-Atlantic Ridge immediately north of the Azores (Table 3). These regional $\Delta\ \delta^{13}C$ maxima are not linked to specific water depths or deep water masses. Hence we assume that the maxima and their underlying actual cause, the local carbon isotopic minima of *C. wuellerstorfi* during the LGM, were in part controlled by increased local fluxes and concentrations of particulate and dissolved organic carbon near the seafloor below the high-productivity zones of the ocean (compare distribution patterns of Figure 4). This influence from local carbon fluxes must be considered as additive to the one exerted by the general CO_2 level of the deep water masses. A similar feature was observed by Kroopnick [1971] for modern $\delta^{13}C$ values below the high-productivity belt of the equatorial Pacific. In this region the lowermost 40 m of the water column are marked by $\delta^{13}C$ values, which are about 0.3‰ lower than those immediately above.

On a global scale the LGM-to-Holocene $\delta^{13}C$ increase below 1500-2000 m water depth averages 0.4-0.5‰, if we disregard the regionally higher values associated with local high fluxes of organic carbon. This corresponds to a total release of about 580-720 Gt C from the deep ocean below 1500-2000 m to the surface ocean and the atmosphere (applying a simple calculation scheme proposed by Duplessy [1982]).

One might expect the stable isotope composition of planktonic foraminifera to record a corresponding decrease in $\delta^{13}C$ from the LGM to the Holocene in order to compensate for the $\delta^{13}C$ enrichment in the deep sea. However, in most cases, such a simple inverse relationship is not observed. The mechanism for paleoproductivity changes discussed below may provide an explanation for the parallel $\delta^{13}C$ variations found in both surface and bottom water near upwelling regions [Sarnthein and Tiedemann, 1988]. Moreover, a parallel shift in planktonic and benthic $\delta^{13}C$ records is observed for downwelling regions of the ocean where fresh, oxygenated deep water has continuously formed through glacial and interglacial times [Duplessy et al., this issue]. The only examples of a reversed $\delta^{13}C$ shift in oceanic deep and surface waters were found in the nutrient depleted, stratified waters of subtropical gyres such as the Sargasso Sea, where the average glacial $\delta^{13}C$ values of planktonic foraminifera from the surface water increased by 0.2‰ [Curry and Crowley, 1987]. Therefore the ^{13}C trends of the surface water parallels that in the underlying intermediate water (Figure 3)[Zahn et al., 1987; Duplessy et al., this issue].

Paleoproductivity Changes Since the LGM

Figures 4a and 4b present the changes in new (export) paleoproductivity (delta P_{new}) from the LGM (average of 17,000-21,000 years B.P.) to the Holocene interglacial (average of the last 8000 years). Difference values were calculated using equation (1) for about 65 deep-sea cores obtained from various key oceanographic regions in the low- and mid-latitude ocean, representing both high and low primary productivity areas. From these few regions we extrapolate to much larger parts of the ocean, for which data is lacking.

Basically, three modes of change since the LGM can be distinguished:

(1) In most regions where modern new production is high, P_{new} was even higher during the LGM. Since the LGM, P_{new} has decreased by 25-80%, which is a factor of up to 5. This reduction occurred along the eastern continental margins of the Atlantic, Pacific, and northwest Indian oceans, off India, and below the equatorial divergence zones of the eastern Pacific, eastern Atlantic, and western Indian oceans. The central equatorial Atlantic forms a slight exception to this rule in that maximum productivity was reached during early stage 2 and started to decrease prior to 20,000 years B.P. (Figure 2g; cores 13521, ENO66-29, and -36). Thus the the central equatorial Atlantic data deviate from the average P_{new} numbers in Figure 4 and Table 3.

A post-glacial productivity decrease is also observed at the few sites from the southern mid-latitude Indian and Atlantic oceans along the glacial position of the Antarctic divergence zone [CLIMAP, 1981]. Likewise, we assume a synglacial divergence zone immediately north of the Azores near 45° N, which led to a local productivity high vanishing during early stage 1 (Figure 2d, core 15612).

(2) In modern low-productivity zones, glacial P_{new} varied in a non systematic way. In wide areas, such as south of

Hawaii, it decreased by 0-50%, similar to the trend found in the high-productivity zones. In many other areas, however, P_{new} increased by up to 200%. This is the case for the unfertile subtropical gyres of both the Pacific and Atlantic oceans (Table 3 and Figures 4a and 4b).

(3) Few regions show a clear reversed trend with a Holocene increase in P_{new}. For example, the increase in P_{new} paralleled the deglacial retreat of perennial sea ice in the Norwegian Sea [Kellogg, 1980] by 35-65%. Furthermore, a productivity increase during Termination I marked the areas immediately offshore from the mouths of the Indus and Senegal rivers, which then started to discharge enormous quantities of nutrients (Figures 2c and 2f, cores 12347 and MD 76-132; Sarnthein et al. [1982b], and Fontugne and Duplessy, [1986]). Finally, offshore from southern Arabia and especially from Yemen, the postglacial increase in P_{new} (Figures 2 and 4) matches the well-known mid-Holocene onset of monsoon-driven coastal upwelling [e.g., Prell and Curry, 1980; Duplessy, 1982].

In most core profiles from the northernmost Arabian Sea, however, the pattern of productivity history appears more complex. Here the distinct mid-Holocene increase in P_{new} was preceded by a short-term decrease of 30-60% near the onset of Termination IA. This productivity low lasted until about 8000 years B.P., the end of Termination IB.

In summary, our data indicate that the small but crucial high-production zones acted in phase with a massive decrease in new production in almost all parts of the low- and mid-latitude ocean during Termination I. A reversed trend is only found in parts of the low-production zones in both the subtropical gyres and the high latitudinal ocean covered by sea ice during the LGM, some narrow prodeltaic areas, and the narrowly confined coastal upwelling zone off southern Arabia. In spite of their wide areal distribution, most of these regions with a reversed trend are not quantitatively important for the global productivity budget as shown on Figure 4b and Tables 3 and 4. The absolute range of production and productivity changes in this regions is much lower or even negligible as compared to the values of the high-productivity belts. Thus we conclude that an overall decrease occurred in the amount of carbon extracted by P_{new} from the low- and mid-latitudinal sea surface to the deep ocean at the end of the last glaciation. Hence low-latitude upwelling and its associated pulsating export productivity must be considered as a strong additional factor, if not the major agent, in changing ocean and atmospheric chemistry during Terminations I and II.

Changes in $\delta^{13}C$ of Organic Matter Parallel to Changes in Ocean Productivity

The $\delta^{13}C$ values of organic matter were reported from a number of sediment cores from coastal upwelling zones off northwest Africa [Müller et al., 1983], India, and south Arabia [Fontugne and Duplessy, 1986] (examples in Figure 5). The values varied between -18‰ and -22‰ from Glacial to Interglacial times. With minor exceptions (e.g., core MD 76-131) the $\delta^{13}C_{org}$ records closely parallel the local fluctuations in new productivity (r=0.84; Figure 5d) and apparently form a little understood isotopic response. Prior to an attempt of interpreting it, we shall discuss what the records may not mean.

The $\delta^{13}C$ range of our limited data set testifies that the organic matter and its downcore variations mainly originate from the marine plankton production and not from the terrigenous input of land plants, the mean isotopic values of which are much lighter ranging near -26‰ $\delta^{13}C$ [Cachier et al., 1986; Fontugne and Duplessy, 1981, 1986]. Furthermore, the $\delta^{13}C_{org}$ values get heavier as the carbon concentrations in the sediment and P_{new} values increase. This is the opposite of what one would expect if the sediments were receiving an increased input of terrestrial organic matter. Also, the exceptionally heavy carbon isotope ratios of some C_4 land plants such as grasses (-13‰) can be ruled out as a possible source for the heavier $\delta^{13}C$ values in our records: typical C:N ratios for grasses range from 20 to 50, whereas those found in the organic matter from sediments below the upwelling region off northwest Africa amount to 8-9, a value characteristic of marine plankton [Suess and Müller, 1980; Müller et al., 1983].

Accordingly, the downcore variations in $\delta^{13}C$ of organic carbon must be related to changes in marine plankton production. Varying sea surface temperatures [Sackett et al., 1965] can also be ruled out as a cause. For example, we must assume an average decrease in sea surface temperatures from 20° to 15°C during the LGM,

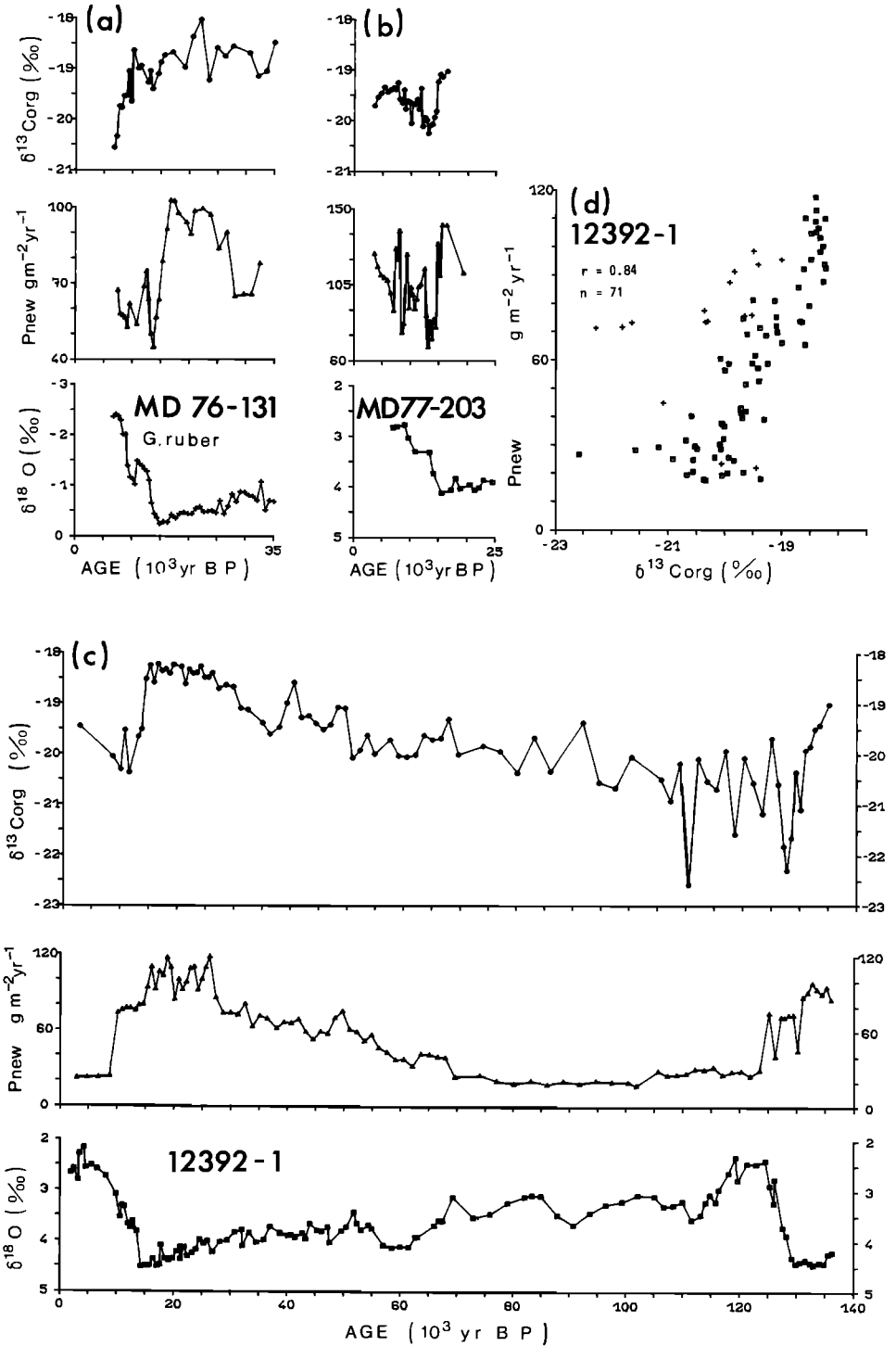

Fig. 5. (a-c) Variations in the carbon isotopic composition (per mill versus PDB) of organic matter versus new paleoproductivity and $\delta^{18}O$ stratigraphy (*C. wuellerstorfi* unless otherwise mentioned) of sediment cores from the east Atlantic and northwest Indian Ocean ($\delta^{13}C_{org}$ data from Müller et al. [1983] and Fontugne and Duplessy [1986]). (d) Correlation between new productivity and $\delta^{13}C$ values of organic matter in Meteor core 12392 (plus signs represent samples from sediment surface and stage 6 subject to diagenetic bias).

when the upwelling intensity and productivity along the east Atlantic continental margin was much enhanced [Sarnthein et al., 1982a]. According to Degens et al. [1968b] and Fontugne and Duplessy [1981], this cooling led to a lowering of the mean $\delta^{13}C$ values of organic matter from about -20 to -22‰. However, our data just exhibit the reversed trend for the LGM, i.e., a rise from -20 to -18‰ (Figure 5, core 12392).

The only modern analogue of the enriched $\delta^{13}C$ values that characterize the organic carbon in sediments from Glacial and Holocene upwelling maxima are data from plankton collected inside (-18.7‰) and outside (20.0‰) of the highly productive Peru upwelling region [Degens et al., 1968a; Reimers and Suess, 1983]. This parallel between high $\delta^{13}C_{org}$ values of marine plankton and high productivity suggests a direct causal link. It might be caused by continued, extensive fractionation of light organic carbon from the CO_2 reservoir near the sea surface. This process might gradually deplete the ^{12}C dissolved in the surface water and result in an increased incorporation of ^{13}C into the organic tissues of marine plankton. Moreover, plankton production might increasingly utilize the isotopically heavier bicarbonate [Degens et al., 1968b; Deuser, 1970]. However, recent experiments on marine phytoplankton cultures [Descolas-Gros and Fontugne, 1985] do not corroborate this model. They suggest that the $\delta^{13}C$ composition of marine algae is independent of the isotopic equilibrium and concentration of total dissolved CO_2 in ambient water. Moreover, Boyle [1986a] reports of a general excess of CO_2 in the surface ocean.

On the other hand, the experiments of Descolas-Gros and Fontugne [1985] provide essential new insights that may help to unravel the puzzling $\delta^{13}C$ response of marine plankton to productivity changes. Their findings suggest two different ways for raising the $\delta^{13}C_{org}$ values, which may overlap. First, they clearly distinguish two phases of monospecific cell growth in the carbon isotopic composition of diatoms. The initial phase of exponential growth produced isotopically light plankton (-23 to -17‰), whereas the second, stationary growth phase of the cell culture (after 2 days) induced a massive $\delta^{13}C_{org}$ rise up to values indicative of C_4 metabolism (-9 to -13‰). Descolas-Gros and Fontugne [1985] surmised that this shift may result from deteriorating growth conditions such as lowered light intensity. However, experiments of Degens et al. [1968b] and measurements of Wefer and Killingley [1986] on algae from the natural environment revealed just the contrary, a decreasing $\delta^{13}C$ trend in algae along with decreasing light intensity. We propose as an alternative explanation that both the shift from exponential to stationary growth and the increase in the $\delta^{13}C$ ratio are due to a drastic depletion of (some portions of) nutrients in the monospecific cell culture after 2 days.

Second, Descolas-Gros and Fontugne [1985] found the increased carbon isotopic ratios clearly linked to the special carbon fixation mechanism [β carboxylation] of dinoflagellates and Chlorophyceae. These groups show characteristically heavier carbon isotopic values (about -18‰) than diatoms (average: -22‰). Since dinoflagellates do not require silicon, they are probably less specialized and capable to cope with less favorable growth environments. After Codispoti [1983] and Codispoti et al. [1982], immense blooms of dinoflagellates, "red tides," are characteristic of the unfavorable chemical conditions of the El Niño phases in the world's strongest coastal upwelling zones such as that off Peru. These unusual conditions comprise: (1) a complete denitrification of the surface water as opposed to subsurface maxima of ammonia, phosphorus, and silicon, i.e., not a general nutrient depletion (except for the thin surface layer) but an unusually low N:P (Redfield) ratio; (2) extreme oxygen deficiency in the subsurface layer associated with H_2S production; and (3) occasional upwelling of H_2S to the warmer surface layer, a process that is poisoning most other organism groups. Hence by means of the dinoflagellates we recognize, once again, a specific deficit in the nutrient budget (in combination with H_2S production) as the prime factor for anomalies in ^{13}C enrichment of organic matter.

Both lines of evidence, especially that of the dinoflagellates, lead to an apparent paradox: maxima in the $\delta^{13}C$ composition of organic matter attest both long-term phases of enhanced new productivity and short-term phases of nutrient (nitrate) depletion in upwelling cells. This discrepancy may be resolved by considering the mechanism proposed by Codispoti [1983]: when (glacial) upwelling systems become "too efficient" and act as nutrient traps, reactive phosphorus and dissolved silicon may continue to increase. How-

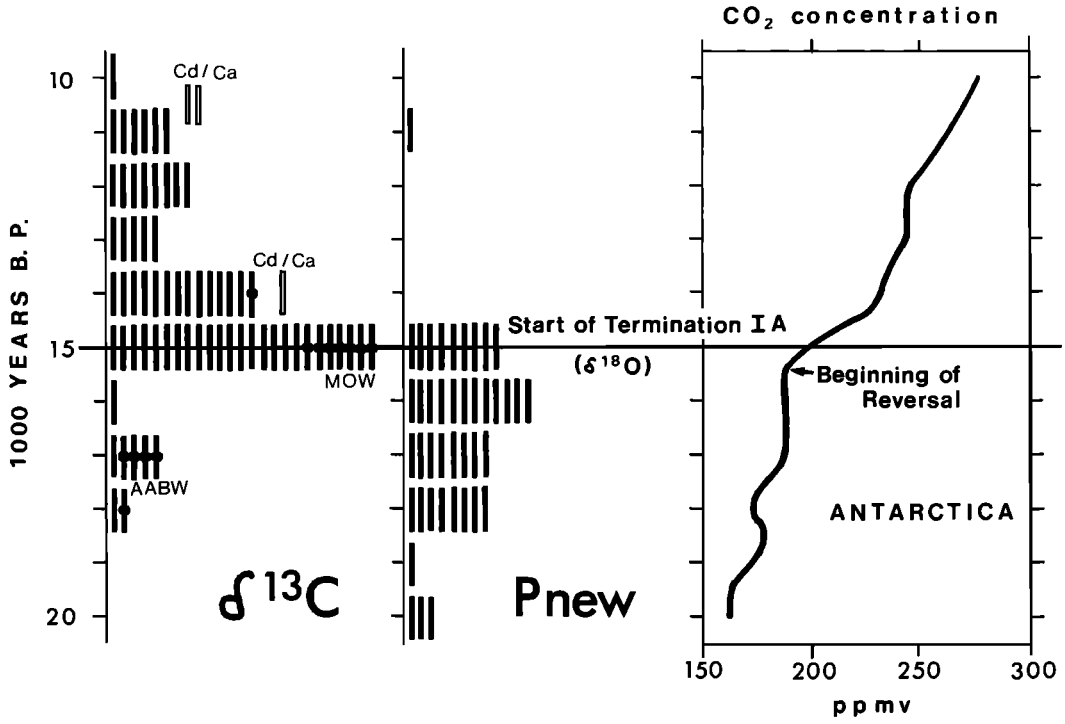

Fig. 6. Lead/lag relationships of onset ages of reversals in paleoproductivity and $\delta^{13}C$ curves versus those in $\delta^{18}O$ curves (Figure 2) during the onset of glacial Termination I, plotted as frequency histographs for 1000-year intervals. Age of 15,000 years B.P. for start of Termination IA in $\delta^{18}O$ curves is best estimate out of numerous radiocarbon datings. Onset ages of reversals in Cd/Ca records (marked in the figure) from Boyle and Keigwin [1985]. Data from Mediterranean Outflow Water (MOW) and Antarctic Bottom Water (AABW) in central Atlantic are marked. Variations in atmospheric pCO_2 from Antarctic ice cores from De Angelis et al. [1984].

ever, nitrate concentrations decrease as a consequence of ongoing denitrification, largely as a result of reduced or inadequate subsurface horizontal advection.

In summary, from both the red tide mechanism in upwelling cells and the ^{13}C enrichment during stationary phases of algal growth we may infer that heavier $\delta^{13}C_{org}$ values record El Niño related denitrification events and that phases of very high [coastal] upwelling productivity always imply strong El Niño cycles. More detailed studies are required for a better understanding of the complicated processes involved.

DISCUSSION

Phase Relationships During Termination I

Figure 6 compares the age of the beginning of reversals found for different paleoceanographic and paleoclimatic curves after the LGM. The figure compares the reversals in benthic $\delta^{13}C$ records of dissolved CO_2 in the deep sea and in the records of (new) paleoproductivity with the onset age of glacial Termination I_A as documented by the turning points in $\delta^{18}O$ curves at 15,000 years B.P. (Figure 2) and with the ice core record of increasing CO_2 concentrations in the atmosphere [De Angelis et al., 1984].

Problems of stratigraphic correlation were largely avoided by using only intracore correlations. Moreover, those between the $\delta^{13}C$ and $\delta^{18}O$ curves rely on data being obtained from the same specimens of *C. wuellerstorfi*. Of course, the results from this single-case phase study cannot be generalized for the phase relationships of other Quaternary climatic cycles. However, the data may well illustrate the succession of processes on a global scale during the last major climatic reversal and by these means, also display some

specific cause and effect relationships with obvious ramifications for the dramatic change in the oceanic and atmospheric CO_2 budgets.

Within the limits of the time control, the CO_2 concentrations measured in polar ice cores began to increase at about 16,000 to 15,000 years B.P. [De Angelis et al. 1984; Lorius et al., 1984; Oeschger et al., 1984, Barnola et al., 1987]. This is synchronous with or slightly prior to the $\delta^{18}O$ shift observed in the same ice cores. On the other hand, in most cases, the $\delta^{13}C$ records indicate that the beginning of CO_2 depletion in the deep sea lags behind the onset of the respective $\delta^{18}O$ shift by about 1000-4000 years (Figure 6).

Only a small number of cores show a synchroneity in the $\delta^{13}C$ and $\delta^{18}O$ signals, with many of them associated with MOW (i.e., they document a local event). Most of the remaining cores with a synchronous carbon and oxygen isotope signal are from areas with low deposition rates and/or with low concentrations of *C. wuellerstorfi* during the LGM. These factors result in strong homogenization through bioturbation or a downcore shift of the benthic $\delta^{13}C$ signal and thus can readily explain reductions in the phase shift between the two isotopic records.

In general, the lags in the $\delta^{13}C$ shift versus that in $\delta^{18}O$ do not vary through the different parts of the ocean, except for a striking lead in the $\delta^{13}C$ signal by about 2000 years in cores from the deep, restricted basins of the equatorial and southern east Atlantic (Figure 6). Their unusually high delta $\delta^{13}C$ values exceed 0.9‰ (Figure 3) and are ascribed to an inflow of particularly ^{13}C depleted deep Antarctic Bottom Water (AABW). Accordingly, this regional lead may indicate either a very early onset of change in the chemistry of the deepest portion of Antarctic Bottom Water advected to these basins or a very early decrease in productivity in the equatorial Atlantic.

The prevailing lag of $\delta^{13}C$ records versus the ice core record of atmospheric pCO_2 matches the one of the Cd/Ca signal (Figure 6), which serves as an independent record of a delayed decrease in dissolved phosphate of the deep ocean [Boyle and Keigwin, 1985]. This sequence of events contradicts the widely accepted model that changes in atmospheric pCO_2 are mainly controlled and/or triggered by variations in deep ocean circulation.

The phase relationship between paleoproductivity and $\delta^{18}O$ is exactly the inverse of that between $\delta^{13}C$ and $\delta^{18}O$. Thus the start of the low- and mid-latitude productivity reduction compares well with the timing of the ice core record of atmospheric pCO_2 change during Termination IA. Both processes continue for the subsequent 5000-7000 years. The onset of the decrease in productivity after the LGM leads the onset of Termination I by up to 5000 years. This phase relationship has important implications for the "shelf effect" model, which contends that the decrease in lateral downslope discharge of organic material to the continental rise due to sea level rise is a possible control of the carbon budget in the deep sea [Walsh et al., 1981]. This process can now be virtually excluded as the major cause for both the reduction in carbon accumulation rates and the increase in $\delta^{13}C$ during early stage 1.

Virtually no case of a productivity phase lead exceeding 3000 years is substantiated in our data. The long leads that do exist are an artifact of a low sampling density. On the other hand, most short-phase leads are associated with the better documented core sections and/or high sedimentation rates. Thus only shorter-phase leads in paleoproductivity reduction are regarded as more reliable.

Moreover, most phase leads may be strongly exaggerated because of the role of bioturbation. As soon as productivity and the flux of carbon to the seafloor decrease, the benthos will start an enhanced consumption, a "burn-down" of "fossil" carbon [Rowe, 1985]. By both this mechanism and subsequent enhanced oxidation of oxygen-depleted deposits, the carbon concentration in the sediment and the resulting paleoproductivity signal can be reduced to depths of about 6-15 cm below the paleosediment surface (i.e., below the core depth of the actual reversal in carbon supply). This depth of bioturbational mixing represents a time span of 1000-5000 years. As a result, the apparent productivity lead under discussion will probably be much reduced. In addition, the total phase lead between paleoproductivity and $\delta^{13}C$ may shrink to a time span of 1000-3000 years.

This model on the extent and impact of bioturbational "burn-down" depth receives independent support from the $\delta^{13}C$ records of organic matter, which are closely linked to the intensity of long-term upwelling productivity (Figure 5). In core 12392 where sedimentation rates are about 10 cm/ 1000 years, the shift in

$\delta^{13}C_{org}$ starts at exactly the same core depth as the $\delta^{18}O$ shift associated with Termination IA, i.e., 15 cm or 1500 years above the onset of the paleoproductivity shift (Figure 5). Thus an actual synchroneity in the onset of ice melt and the decrease of upwelling productivity appears more likely than a lead in paleoproductivity. Similar relationships are observed between the $\delta^{13}C_{org}$ curves and paleoproductivity shifts in other cores. Meridional trade winds probably play a crucial role as a transmission belt for the rapid teleconnection of high-latitude deglaciation and low-latitude decrease in upwelling productivity as discussed in detail by Sarnthein et al. [1987].

In summary, we can make the following observations:

During Termination IA, wind-driven upwelling productivity began to decrease across large parts of the low-and mid-latitude ocean slightly prior to or simultaneously with the onset of the global warming and ice melting. The decrease continued (in two steps) for about 5000-7000 years (Figure 2).

The process of decreasing carbon extraction from the surface ocean occurred almost simultaneously with the rapid increase in atmospheric pCO_2. Also, El Niño type events that occasionally depleted nitrate in coastal upwelling zones as suggested by $\delta^{13}C$ records of organic matter immediately ended abruptly at this time.

The much larger and more sluggish CO_2 reservoir in the deep ocean started to respond to the paleoproductivity reduction with a delay of 1000 years or more. Also, the gradual CO_2 depletion of the deep water continued for about 5000 years.

Implications for CO_2 Cycling Between Deep Ocean and Atmosphere

As shown on Figure 3, the deep ocean below 1500-2000 m showed an average ^{13}C increase of about 0.4-0.5‰ $\delta^{13}C$ during Termination I, which is equal to a loss of 580-720 Gt C during about 5000 years. This change started at least 1000 years after the simultaneous onset of the increase in atmospheric pCO_2 and a 25-80% reduction in new production in most of the highly productive upwelling zones (Figures 4 and 6). Thus we infer that the transfer of particulate carbon from low- and mid-latitude upwelling zones has largely contributed to the change of the deep ocean and atmospheric pCO_2, as was proposed by the Rain-Ratio model of Berger and Keir [1984] and by model calculations of Dymond and Lyle [1985] and Boyle [1986a].

In the following we quantitatively estimate the changes in the exchange of oceanic and atmospheric CO_2 during Termination I based on our data and the following assumptions:

1. The deglacial reduction in calcium carbonate production, that is, the decreasing supply of alkalinity to the deep ocean linked to decreasing paleoproductivity, can be largely neglected in our calculations for two reasons: (1) The "rain ratio" between carbonate carbon and organic carbon is as low as 0.16-0.1 in the high-productivity regions and has distinctly increased with decreasing productivity and increasing temperatures [Berger and Keir, 1984; Dymond and Lyle, 1985]; and (2) an eventual minor postglacial decrease in carbonate production within the upwelling zones will be partly balanced by a synchronous productivity growth found outside, in some warm, low-latitudinal low-productivity regions of the ocean where the "rain ratio" is about 1 (e.g., Sierra Leone Rise; Curry and Lohmann [1984]).

2. Recent reconstructions of the paleo-deep-water circulation in the Atlantic during the LGM [Broecker, 1987; Duplessy et al., this issue; JS, 1988] show a persistent source of Antarctic Bottom Water and a continuous, but somewhat reduced formation of North Atlantic Deep Water. Thus the impact of circulation changes on the CO_2 budget during the LGM is likely but smaller in magnitude than originally suggested [e.g., Broecker, 1984].

3. The estimates and distribution patterns of primary production in the modern ocean as published by Koblentz-Mishke et al. [1970] (improved version in the work of FAO [1981] and Romankevich [1984]) and by De Vooys [1977] are regarded as the best approximations available.

4. We accept that the equation of Eppley and Peterson [1979] is widely settled. This implies that the proportion of new (export) production in the total production increases exponentially from low- to high-productivity regions. On a global average, new production may amount to about one third of total production [Platt and Harrison, 1985].

5. The nutrient pool probably did not seriously limit a major glacial increase

TABLE 4a. Balance of Changes in New Productivity, Based on Estimates of Koblentz-Mishke et al. [1970]

Oceanic Regions	Area $10^6 km^2$/ %	Modern Primary Production Rates		Modern Primary Production		% Average Decrease in P_{new} since LGM[1]	P_{new} LGM, Gt C/yr
		Total, g/m^2 yr	New,[5] g/m^2 yr	Total, Gt C/yr %	New,[5] Gt C/yr %		
1. Neritic waters	11/ 3.0	365.0	182.5	3.9 / 17.0	1.95/ 36.0	?0 ?-110[2]	?1.95
2. Coastal waters	39/ 10.6	124.0	38.5	4.8 / 21.0	1.5 / 27.8	(40-80)[3]	3.0
3a. Equatorial divergence	43/ 11.7	73.0	13.5	3.15/ 13.7	0.58/ 10.7	(35-50)[3]	1.0
3b. Subpolar zones	43/ 11.7			3.15/ 13.7	0.57/ 10.6	(13-93)[4]	0.65-1.15
	37.0			15.0 / 65.2	4.6 / 85.2	(50)	6.6 -7.1
4. Transitional waters	83/ 22.7	51.0	6.5	4.2 / 18.3	0.55/ 10.2	-(20-80) -(50)	0.37
5. Oligotrophic waters	148/ 40.3	25.6	1.65	3.8 / 16.5	0.25/ 4.6	(13-31) (22)	0.33
(subtropical gyres)	63.0			8.0 / 34.8	0.8 / 14.8		0.7
	100.0			23.0 /100.0	5.4 /100.0	(33-37	7.3 -7.8

[1] Compare Table 1 and Figure 3

[2] Few values available. In subtropical regions, possibly reduced during LGM due to reduced chemical weathering. In Mediterranean latitudes, possibly increased, i.e., in total, no change.

[3] Key regions of change well documented.

[4] Few values available. LGM to Holocene decrease at 45°N: >90%; at 45-55°S: 13.5-68%. Lower estimate is more probable because of lower production in polar latitudes during LGM.

[5] Applying equation (2) of Eppley and Peterson [1979] to average values of P_{total}.

in upwelling productivity in middle and low latitudes. Sufficient nutrients are supplied by intermediate water currents. They spread below the thermocline at 100-1000 m depth from the convergence zones in southern high latitudes far into the northern hemisphere. During glacial times, they provided an efficient mechanism to redistribute additional nutrients from (mostly southern) high latitudes that were sea ice covered and free of production. For example, the South Atlantic Central Water has fed east Atlantic upwelling up to 26°N [Fraga, 1974; Labracherie, 1980; Tomczak, 1984]. Likewise, intermediate water currents play an important role in east Pacific and Indian ocean upwelling [Codispoti, 1981]. Hence the (wind-driven) turnover rates of the surface ocean and its nutrient content are regarded as largely decoupled from the long-term, slow upward nutrient flux in the deep ocean, which is driven by vertical eddy diffusivity and general horizontal deep water ventilation.

According to the estimates of Koblentz-Mishke et al. [1970] and Romankevich [1984], the total modern primary production of organic carbon in the ocean amounts to 23 Gt carbon/year (Table 4a). About two thirds of this sum are derived from one third of the ocean. This uneven distribution is far more pronounced in the budget of new production (in total 5.4 Gt carbon/year). It extracts less than 5% of the total organic carbon from oligotrophic waters constituting 40% of the sea surface but about 85% from narrow high-productivity belts along the equator, the subpolar divergence zones, and along the continental margins (regions 1-3 on Table 4a). In comparison, Jahnke and Jackson [1987] claim that as much as 50% of all the benthic oxygen consumption is concentrated in regions within 500 km distance from continental margins.

Table 4b. Balance of Changes in New Productivity, Based on Estimates of De Vooys [1977]

Oceanic Regions	Area $10^6 km^2$/ %	Modern Primary Production Rates: Total, g/m^2 yr	Modern Primary Production Rates: New,[5] g/m^2 yr	Modern Primary Production: Total, Gt C/yr %	Modern Primary Production: New,[5] Gt C/yr %	% Average Decrease in P_{new} since LGM[1]	P_{new} LGM, Gt C/yr
1. Neritic waters	11/ 3.0	527.0	264.0	5.6 / 17.0	2.8 / 28.3	?0 ?-110[2]	?2.8
2. Coastal waters	39/ 10.6	179.0	80.1	6.9 / 21.0	3.1 /31.3	(40-80)[3]	6.2
3a. Equatorial divergence	43/ 11.7			4.55/ 13.7	1.2 /12.1	(35-50)[3]	2.1
		105.4	27.8				
3b. Subpolar zones	43/ 11.7			4.55/ 13.7	1.2 / 12.1	(13-93)[4]	1.37-2.4
	37.0			30.7 / 65.2	8.3 / 83.8	(50)	12.5-13.5
4. Transitional waters	83/ 22.7	73.7	13.6	6.05/ 18.3	1.1 / 11.2	-(20-80) -(50)	0.55
5. Oligotrophic waters	148/ 40.3	37.0	3.4	5.5 / 16.5	0.5 / 5.1	(13-31) (22)	0.6
(subtropical gyres)	63.0			11.55/ 34.8	1.6 / 16.2		1.35
	100.0			33.2 /100.0	9.9 /100.0	(40-50)	13.8-14.9

[1] Compare Table 3 and Figure 5

[2] Few values available. In subtropical regions possibly reduced during LGM due to reduced chemical weathering. In Mediterranean latitudes possibly increased, i.e., in total, no change.

[3] Key regions of change well documented.

[4] Few values available. LGM to Holocene decrease at 45°N: >90%; at 45-55°S: 13.5-68%. Lower estimate is more probable because of lower production in polar latitudes during LGM.

[5] Applying equation (2) of Eppley and Peterson [1979] to average values of P_{total}.

The same narrow regions are also expected to be crucial for any budget changes during the past. Global productivity estimates of De Vooys [1977], which claim for an upward correction of the values of Koblentz-Mishke et al. [1970] by at least 44%, reveal the same uneven regional distribution pattern but raise the global sum of new production by about 85% to 9.9 Gt carbon/year (Table 4b).

Based on the estimates of Koblentz-Mishke et al. [1970] and a conservative evaluation of our data, P_{new} reached a global sum of 7.3-7.8 Gt carbon/year during the LGM, which means 1.9-2.4 Gt carbon/year more than today (Table 4a). Based on De Vooys [1977], P_{new} amounted to 13.8-14.85 Gt carbon/year during the LGM, i.e., 3.9-5.0 Gt carbon or 40-50% more than today (Table 4b). This increase in productivity occurred primarily in upwelling regions with frequent events of plankton blooms (Table 2), and we surmise that it was largely wind-driven [Sarnthein et al., 1987]. If persistent over prolonged periods, the difference in Pnew might readily account for the observed glacial-to-interglacial loss of about 650 Gt carbon from the deep to the surface ocean and atmosphere within a time span of less than 300 or 150 years, respectively. In reality the response of the deep ocean was delayed by more than 1000 years. From these data it is not surprising that new ice core data [Barnola et al., 1987] exhibit an increase in the atmospheric CO_2 content by about 150 Gt carbon in less than 1000 years.

Changes in sea surface temperature paralleling the variations in upwelling productivity will further enhance the effect of P_{new} changes on pCO_2 [Newell et al., 1978; Flohn, 1982]. Glacial phases of strong upwelling produced a local lowering of sea surface temperatures by up to 4°-8°C [CLIMAP, 1981], which in turn reduced the physical degassing of excess CO_2 at the sea surface. This effect may counter-

act that of enhanced glacial turnover rates of upwelling water masses, a process which several models suggest as a crucial constraint for the CO_2 exchange in low latitudes [e.g., Toggweiler and Sarmiento, 1985; W. S. Broecker, personal communication, 1987].

CONCLUSIONS

1. Based on $\delta^{13}C$ estimates of the benthic foraminifera species *C. wuellerstorfi*, the average $\delta^{13}C$ values in the deep ocean below 1500 (to 2000) m increased by 0.4-0.5‰ from the last LGM (17,000-21,000 years B.P.) to the Holocene (last 8,000 years). This rise equates to a release of about 580-720 Gt carbon from the deep to the surface ocean and to the atmosphere.

2. The $\delta^{13}C$ values of intermediate waters in the north Atlantic decreased by up to 0.2-0.5‰ from glacial to interglacial times. Off southern Greenland at about 1850 m depth and deeper, enriched $\delta^{13}C$ values reveal the formation of oxygen-rich NADW during the LGM [Duplessy et al., this issue]. At 1000-1600 m water depth in mid and low latitudes they indicate an increased synglacial supply of both North Atlantic Intermediate Water and well-oxygenated Mediterranean Water [Zahn et al., 1987].

3. Glacial to interglacial $\delta^{13}C$ differences increased by 0.2-0.5‰ to values of 0.5-0.9‰ in regions where the productivity of the LGM surface ocean was strongly enhanced. We relate this additional ^{13}C depletion during the last LGM to local high concentrations of isotopically light organic carbon near the seafloor. More extreme $\delta^{13}C$ differences of 0.9->1.2‰ occur in the deep basins of the southeastern Atlantic and record a synglacial advection of ^{12}C enriched AABW below 4000-4500 m water depth.

4. Based on carbon accumulation rates derived from a global set of 65 deep-sea cores, the rates of global new (export) ocean production (P_{new}) declined by more than 2-4 Gt carbon/year during the last glacial Termination. To a large extent, this decrease was linked to diminished carbon export from pulsating plankton blooms and resulted from a strong reduction in oceanic upwelling in middle and low latitudes.

5. At the onset of deglaciation the rise in atmospheric pCO_2 as recorded in ice cores and the decrease in paleoproductivity started about simultaneously with a decrease in the strength of meridional surface (trade) winds [Sarnthein et al., 1987] and slightly prior to the $\delta^{18}O$ record of glacial melting. On the other hand, benthic $\delta^{13}C$ curves show that the onset of large-scale CO_2 emission from the deep ocean was delayed by 1000 years and more.

6. It is likely that fluctuations of mid- and low-latitude P_{new} have largely controlled the changes in ocean and atmospheric chemistry, whereas the deep ocean chemistry slowly responded to the differential fluxes of particulate organic matter. Variations in P_{new} are likely to form a highly sensitive response to the external forcing of the Earth's orbital parameters because P_{new} changes are driven by meridional surface winds, which in turn are linked to the extent of high-latitude sea ice and insolation. If persistent over prolonged periods, changes in paleoproductivity in theory could drive the glacial-to-interglacial changes in atmospheric pCO_2 within 150-300 years. This model is in harmony with those originally proposed by Newell et al. [1978] and Flohn [1982].

7. The glacial maximum of P_{new} in upwelling zones is highly correlated to an increase in the $\delta^{13}C$ ratio of organic matter by up to 2‰. This increase may be due to immense dinoflagellate plankton blooms associated with El Niño type events of local denitrification. In the modern east Pacific [Codispoti, 1983] they may result from an extreme utilization of the ambient nutrient reservoirs in glacial coastal upwelling cells, which became "too efficient" and acted as nutrient traps.

Acknowledgements. The authors are most appreciative of the valuable and critical comments from a number of colleagues, in particular, M. Arthur, M. Leinen, W. S. Broecker, and T. Takahashi, when the first author (M.S.) spent a sabbatical leave at the University of Rhode Island, Narragansett, and the Lamont-Doherty Geological Observatory, New York, with the support of funds from the Deutsche Forschungsgemeinschaft, Bonn. We thank an anonymous careful reviewer and John Schumacher for their numerous valuable improvements on the manuscript. N. J. Shackleton, Cambridge, United Kingdom, L. Peterson (Miami, formerly of Brown University), J. H. F. Jansen (Texel), R. Zahn-Knoll (Oregon State University, Corvallis, formerly Kiel), M. Hartmann, H. Kassens, F.

Sirocko, and E. Vogelsang (Christian-Albrechts-Universität, Kiel) kindly provided unpublished $\delta^{13}C$ and sediment data from the Indian and the eastern and northern Atlantic oceans, T. Pedersen (Vancouver) supplied core samples and carbon data from the eastern equatorial Pacific. U. Pflaumann (Kiel) assisted with the supply of valuable computer software. Both the Bundesanstalt für Geowissenschaften und Rohstoffe and the PREUSSAG, Hannover, permitted extensive sampling of their sediment cores from the Pacific ocean. This work was generously supported by fundings from the National Climate Project of the German Federal Ministry for Research and Technology (BMFT), grant KF 2004/1 and by the French Centre Nationale de la Récherche Scientifique - Commissariat de l'Energie Atomique (CNRS-CEA), Groupement de Récherche Coordinés Carbon Dioxide (Programme Interdisciplinaire de Récherche sur Environment) (GRECO CO_2 (PIREN)), and Terre Austral et Antarctique Francaise (TAAF). This paper is in honor of E. Seibold on the occasion of his 70th birthday.

REFERENCES

Altenbach, A., and M. Sarnthein, Productivity record in benthic foraminifera, in *Dahlem Konferenzen, Physical, Chemical, and Earth Sciences Research Report*, (in press), 1988.

Bard, E., M. Arnold, J. Duprat, J. Moyes, and J. -C. Duplessy, Reconstruction of the last deglaciation: deconvolved records of $\delta^{18}O$ profiles, micropaleontological variations and accelerator mass spectrometric ^{14}C dating, *Climate Dyn., 1*, 101-112, 1987.

Barnola, J. M., D. Raynaud, Y. S. Korotkevich, and C. Lorius, Vostok ice core provides 160,000-year record of atmospheric CO_2, *Nature, 329*, 408-414, 1987.

Berger, W. H., and R. S. Keir, Glacial-Holocene changes in atmospheric CO_2 and the deep-sea record, in *Climate Processes and Climate Sensitivity, Geophys. Monogr. Ser.*, vol. 29, edited by J. E. Hansen and T. Takahashi, pp. 337-351, Washington, D.C., 1984.

Berger, W. H., and E. Vincent, Deep-Sea Carbonates: Reading the carbon-isotope signal, *Geol. Rundsch., 75*, 249-270, 1986.

Betzer, R. R., W. J. Showers, E. A. Laws, C. D. Winn, G. R. Di Tullio, and P. M. Kroopnick, Primary productivity and particle fluxes on a transect of the equator at 153°W in the Pacific Ocean, *Deep Sea Res., 31*, 1-11, 1984.

Bishop, J. K. B., and J. Marra, Variations in primary production and particulate carbon flux through the base of the euphotic zone at the site of the Sediment Trap Intercomparison Experiment (Panama Basin), *J. Mar. Res., 42*, 189-206, 1984.

Boyle, E. A., Deep ocean circulation, preformed nutrients, and atmospheric carbon dioxide: theories and evidence from oceanic sediments, in *Mesozoic and Cenozoic Oceans, Geodyn. Ser.*, vol. 15, edited by K. J. Hsü, pp. 49-59, AGU, Washington, D.C., 1986a.

Boyle, E. A., Paired cadmium and carbon isotope data in benthic foraminifera: Implications for changes in oceanic phosphorus, oceanic circulation, and atmospheric carbon dioxide, *Geochem. Cosmochim. Acta, 50*, 265-276, 1986b.

Boyle, E. A., and L. D. Keigwin, Comparison of Atlantic and Pacific paleochemical records for the last 215,000 years: Changes in deep ocean circulation and chemical inventories, *Earth Planet. Sci. Lett., 76 (1/2)*, 135-150, 1985.

Boyle, E. A., and L. D. Keigwin, North Atlantic thermohaline circulation during the last 20,000 years: Link to high-latitude surface temperature, *Nature, 330*, 35-40, 1987.

Brewer, P. G., K. W. Bruland, R. W. Eppley, and J. J. McCarthy, The Global Ocean Flux Study (GOFS): Status of the U.S. GOFS Program, *Eos Trans. AGU, 67 (44)*, 827-832, 1986.

Broecker, W. S., Glacial to interglacial changes in ocean chemistry, *Prog. Oceanogr., 11*, 151-197, 1982.

Broecker, W. S., Carbon cycle: Carbon dioxide circulation through ocean and atmosphere, *Nature, 308*, 602, 1984.

Broecker, W. S., Palaeoocean circulation rates as determined from accelerator radiocarbon measurements on hand-picked foraminifera, *Terra cognita, 7*, 43-44, 1987.

Broecker, W. S., A. Mix, M. Andree, and H. Oeschger, Radiocarbon measurements on coexisting benthic and planktic foraminifera shells: potential for reconstructing ocean ventilation times over the past 20,000 years, *Nucl. Instrum. Methods Phys. Res., B5*, 331-339, 1984.

Broecker, W.S., and T. Takahashi, Is there a tie between atmospheric CO_2 content and ocean circulation?, in *Climate Pro-*

cesses and Climate Sensitivity, Geophys. Monogr. Ser., vol. 29, edited by J. E. Hansen and T. Takahashi, AGU, Washington, D. C., pp. 314-326, 1984.

Broecker, W. S., D. M. Peteet, and D. Rind, Does the ocean-atmosphere system have more than one stable mode of operation?, *Nature, 315,* 21-26, 1985.

Broecker, W. S., and T. -H. Peng, Carbon Cycle: 1985. Glacial to interglacial changes in the operation of the global carbon cycle, *Radiocarbon, 28,* 309-327, 1986.

Cachier, H., P. Buat-Menard, M. Fontugne, and R. Chesselet, Long-range transport of continentally-derived particulate carbon in the marine atmosphere: Evidence from stable carbon isotope studies, *Tellus, 38B,* 161-177, 1986.

CLIMAP Project Members, Seasonal reconstructions of the Earth's surface at the last Glacial maximum, *Chart Ser. MC-36,* Geol. Soc. of Am., Boulder, Colo., 1981.

Cochran, J. K., Particle mixing rates in sediments of the eastern equatorial Pacific: Evidence from ^{210}Pb, $^{239,240}Pu$ and ^{137}Cs distributions at MANOP sites, *Geochim. Cosmochim. Acta, 49,* 1195-1210, 1985.

Codispoti, L. A., Temporal nutrient variability in three different upwelling regions, in *Coastal Upwelling, Coastal Estuarine Sci. Ser.* , vol. 1, edited by F. A. Richards, pp. 209-220, AGU, Washington D. C., 1981.

Codispoti, L. A., On nutrient variability and sediments in upwelling regions, in *Coastal Upwelling, its Sediment Record,* Part A, edited by E. Suess and J. Thiede, pp. 125-145, Plenum, New York, 1983.

Codispoti, L. A., R. C. Dugdale, and H. J. Minas, A comparison of the nutrient regimes off Northwest Africa, Peru and Baja California, *Rapp. P. v. Réun, Cons. Int. Explor. Mer., 180,* 184-201, 1982.

Curry, W. B., and G. P. Lohmann, Carbon deposition rates and deep water residence time in the equatorial Atlantic Ocean throughout the last 160,000 years, in *The Carbon Cycle and Atmospheric CO_2: Natural Variations Archean to Present, Geophys. Monogr. Ser.*, vol. 32, edited by E. T. Sundquist and W. S. Broecker, pp. 285-301, AGU, Washington D. C., 1985.

Curry, W. B., and T. J. Crowley, $\delta^{13}C$ in equatorial Atlantic surface waters: Implications for Ice Age pCO_2 levels, *Paleoceanography, 2,* 489-517, 1987.

De Angelis, M., J. Jouzel, C. Lorius, L. Merlivat, J. R. Petit, and D. Raynaud, Ice age data for climate modelling from an Antarctic (Dome C) ice core, in *New Perspectives in Climate Modelling,* edited by A. L. Berger and C. Nicolis, pp. 23-45, Elsevier Science, New York, 1984.

Degens, E. T., R. R. L. Guillard, W. M. Sackett, and J. A. Hellebust, Metabolic fractionation of carbon isotopes in marine plankton, I, Temperature and respiration experiments, *Deep Sea Res., 15,* 1-9, 1968a.

Degens, E. T., M. Behrendt, B. Gotthardt, and E. Reppmann, Metabolic fractionation of carbon isotopes in marine plankton, II, Data on samples collected off the coast of Peru and Ecuador, *Deep Sea Res., 15,* 11-20, 1968b.

Delmas, R. J., J. M. Ascesio, and M. Legrand, Polar ice evidence that atmospheric CO_2 20,000 years B.P. was 50% of present, *Nature, 284,* 155-157, 1980.

Descolas-Gros, C., and M. R. Fontugne, Carbon fixation in marine phytoplankton: carboxylase activities and stable carbon isotope ratios; physiological and paleoclimatological aspects, *Mar. Biol., 87,* 1-6, 1985.

Deuser, W. G., Isotopic evidence for diminishing supply of available carbon during a diatom bloom in the Black Sea, *Nature, 225,* 1069, 1970.

De Vooys, C. G. N., Primary production in aquatic environments, in *The Global Carbon Cycle, Scope 13,* edited by B. Bolin et al., pp. 259-292, John Wiley, New York, 1977.

Duplessy, J. -C., Isotope studies, in *Climatic Change,* vol. 3, edited by J. Gribbin, pp. 46-67, Cambridge University Press, Cambridge, United Kingdom, 1978.

Duplessy, J. -C., North Atlantic Deep Water circulation during the last climatic cycle, *Bull. Inst. Geol. Bassin Aquitaine Bordeaux, 31,* 379-391, 1982.

Duplessy, J. -C., G. Delibrias, J. L. Turon, C. Pujol and J. Duprat, Deglacial warming of the paleoclimatic evolution of the European continent, *Palaeogeogr. Palaeoclimatol. Palaeoecol., 35,* 121-144, 1981.

Duplessy, J. -C., N. J. Shackleton, R. K. Matthews, W. Prell, W. F. Ruddiman, M. Caralp, and C. H. Hendy, ^{13}C record of benthic foraminifera in the last Interglacial ocean: Implications for the carbon cycle and the global deep water circulation, *Quat. Res., 21,* 244-263, 1984.

Duplessy, J. -C., and N. J. Shackleton, Response of global deep-water circula-

tion to Earth's climatic change 135,000-107,000 years ago, *Nature, 316,* 500-507, 1985.

Duplessy, J. -C., N. J. Shackleton, R. Fairbanks, L. Labeyrie, D. Oppo, and N. Kallel, Deep water source variations during the last climatic cycle and their impact on the global deep-water circulation, *Paleoceanography,* this issue.

Dymond, J., and M. Lyle, Flux comparisons between sediments and sediment traps in the eastern tropical Pacific: Implications for CO_2 variations dueing the Pleistocene, *Limnol. Oceanogr., 30,* 699-712, 1985.

Eppley, R., and B. J. Peterson, Particulate organic matter flux and planktonic new production in the deep ocean, *Nature, 282,* 677-680, 1979.

FAO Fisheries Department, Atlas of the living resources of the seas, Food and Agricultural Organisation, Rome, 4th ed., 1981.

Flohn, H., Oceanic upwelling as a key for abrupt climatic change, *J. Meteorol. Soc. Jpn., 60,* 268-273, 1982.

Fontugne, M. R., and J. -C. Duplessy, Organic carbon isotopic fractionation by marine plankton in the temperature range -1° to 31°C, *Oceanol. Acta, 4,* 85-90, 1981.

Fontugne, M. R., and J. -C. Duplessy, Variations of the monsoon regime during the upper Quaternary: evidence from carbon isotopic record of organic matter in North Indian Ocean sediment cores, *Palaeogeogr. Palaeoclimatol. Palaeoecol., 56,* 69-88, 1986.

Fraga, F., Distribution des masses d'eau dans l'upwelling de Mauretanie, *Tethys, 6,* 5-10, 1974.

Ganßen, G., Dokumentation von küstennahem Auftrieb anhand stabiler Isotope in rezenten Foraminiferen vor Nordwest-Afrika, *"Meteor" Forschungsergebn., Reihe C, 37,* 1-46, 1983.

Garcon, V., L. Martinon, J. F. Minster, and C. Provost, Gaining insight into dynamics of CO_2 fluxes in the tropical Atlantic Ocean, *Eos Trans. AGU, 67, (44),* 1041, 1986.

Graham, D. W., B. H. Corliss, M. L. Bender, and L. D. Keigwin jr., Carbon and oxygen isotopic disequilibria of Recent deep-sea benthic foraminifera, *Mar. Micropaleontol., 6,* 483-497, 1981.

Grassl, H., E. Maier-Reimer, E. T. Degens, S. Kempe, and A. Spitzy, CO_2, Kohlenstoff-Kreislauf und Klima, I, Globale Kohlenstoffbilanz, *Naturwissenschaften, 71,* 129-136, 1984.

Hartmann, M., P. J. Müller, E. Suess, and C. H. van der Wejden, Chemistry of Late Quaternary sediments and their interstitial waters from the northwest African continental margin, *"Meteor" Forschungsergebn. Reihe C, 24,* 1-67, 1976.

Honjo, S., Study of ocean fluxes in time and space by bottom-tethered sediment trap arrays, A recommendation, in *Global Ocean Flux Study, Proceedings of a workshop,* pp. 305-324, National Academy Press, Washington D. C., 1984.

Honjo, S., S. J. Manganini, and J. J. Cole, Sedimentation of biogenic matter in the deep ocean, *Deep Sea Res., 29,* 609-625, 1982.

Jahnke, R. A., and G. A. Jackson, Role of sea floor organismus in oxygen consumption in the deep North Pacific Ocean, *Nature, 329,* 621-623, 1987.

Jansen, J. H. F., T. C. E. van Weering, R. Gides, and J. van Iperen, Middle and Late Quaternary oceanography and climatology of the Zaire-Congo fan and the adjacent eastern Angola Basin. *Neth. J. Sea Res., 17 (2-4),* 201-249, 1984.

Jenkins, W. J., Oxygen utilization rates in North Atlantic subtropical gyre and primary production in oligotrophic systems, *Nature, 300,* 246-248, 1982.

Karl, D. M., and G. A. Knauer, Vertical distribution, transport, and exchange of carbon in the northeast Pacific Ocean: evidence of multiple zones of biological activity, *Deep Sea Res., 31,* 221-243, 1984.

Keigwin, L. D., North Pacific deep water formation during the latest glaciation, *Nature, 330,* 362-365, 1987.

Kellogg, T. B., Paleoclimatology and paleo-oceanography of the Norwegian and Greenland seas: glacial-interglacial contrasts, *Boreas, 9,* 115-137, 1980.

Koblentz-Mischke, O. J., V. V. Volkovinsky, and J. G. Kabanova, Plankton primary production of the World Ocean, in *Scientific Exploration of the South Pacific,* edited by W. S. Wooster, pp. 183-193, National Academy of Science, Washington D. C., 1970.

Kroopnick, P., Oxygen and carbon in the oceans and atmosphere: Stable isotopes as tracers for consumption, production and circulation models, Ph. D. thesis, Univ. of Calif., San Diego, 1971.

Labracherie, M., Les radiolaires temoins de l'évolution hydrologigue depuis le dernier maximum glaciaire au large du Cap Blanc (Afrique du Nord-Ouest), *Palaeogeogr. Palaeoclimatol. Palaeoecol., 32,* 163-184, 1980.

Lorenzen, C. J., N. A. Welshmeyer, and A. E. Copping, Particulate organic carbon flux in the subarctic Pacific, *Deep Sea Res., 30,* 639-643, 1983.

Lorius, C., D. Raynaud, J. R. Petit, J. Jouzel, and L. Merlivat, Last Glacial Maximum-Holocene atmospheric ice-core studies, *Ann. Glaciol., 5,* 88-94, 1984.

Lutze, G. F., and H. Thiel, *Cibicidoides wuellerstorfi* and *Planulina ariminensis,* elevated epibenthic foraminifera, *Ber. Sonderforschungsbereich 313, 6,* pp. 17-30, Christian-Albrechts-Universität, Kiel, 1987.

Lyle, M., D. W. Murray, B. P. Finney, J. Dymond, J. M. Robbins, and K. Brooksforce, The record of Late Pleistocene biogenic sedimentation in the eastern tropical Pacific Ocean, *Paleoceanography, 3,* 39-59, 1988.

Mix, A. C., and R. G. Fairbanks, North Atlantic surface-ocean control of Pleistocene deep-ocean circulation, *Earth Planet. Sci. Lett., 73,* 231-243, 1985.

Morris, R. J., M. J. McCartney, and P. P. E. Weaver, Sapropelic deposits in a sediment core from the Guinea Basin, South Atlantic, *Nature, 309,* 611-614, 1984.

Müller, P. J., and A. Mangini, Organic carbon decomposition rates in sediments of the Pacific manganese nodule belt dated by ^{230}Th and ^{231}Pa, *Earth Planet. Sci. Lett., 51,* 94-114, 1980.

Müller, P. J., and E. Suess, Productivity, sedimentation rate, and sedimentary organic matter in the oceans, I, Organic carbon preservation, *Deep Sea Res., 26,* 1347-1362, 1979.

Müller, P. J., H. Erlenkeuser, and R. von Grafenstein, Glacial to interglacial changes in oceanic productivity inferred from organic carbon cycles in Eastern North Atlantic sediment cores, in *Coastal Upwelling, its Sediment Record,* Part B, edited by E. Suess and J. Thiede, pp. 365-398, Plenum, New York, 1983.

Neftel, A., H. Oeschger, J. Schwander, B. Stauffer, and R. Zumbrunn, Ice core sample measurements give atmospheric CO_2 content during the past 40,000 years, *Nature, 295,* 220-223, 1982.

Newell, R. E., and J. Hsuing, Sea surface temperature, atmospheric CO_2 and the global energy budget: Some comparisons between the past and present, in *Climatic Changes on a Yearly to Millenial Basis,* edited by N. -A. Mörner and W. Karlen, pp. 533-561, D. Reidel, Dordrecht, Holland, 1984.

Newell, R. E., A. R. Navato, and J. Hsiung, Long-term global sea surface temperature fluctuations and their possible influence on atmospheric CO_2 concentrations, *Pure Appl. Geophys., 116,* 351-371, 1978.

Oeschger, H., J. Beer, B. Siegenthaler, W. Stauffer, W. Dansgaard, and C. C. Langway, Late glacial climate history from ice cores, in *Climatic Processes and Climate Sensitivity, Geophys. Monogr. Ser.,* vol. 29, edited by J. E. Hansen and T. Takahashi, pp. 299-306, AGU, Washington D. C., 1984.

Olausson, E., Oxygen and carbon isotope analyses of a Late Quaternary core in the Zaire (Congo) fan, *Neth. J. Sea Res., 17,* 276-279, 1984.

Paterne, M., F. Guichard, J. Labeyrie, P. Y. Gillot, and J. -C. Duplessy, Tyrrhenian Sea tephrachronology of the oxygen isotope record for the past 60,000 years, *Mar. Geol., 72,* 259-286, 1986.

Pedersen, T. F., M. Pickering, J. S. Vogel, N. J. Southon, and D. E. Nelson, The response of benthic foraminifera to productivity cycles in the eastern equatorial Pacific: faunal and geochemical constraints on glacial bottom-water oxygen levels, *Paleoceanography, 3,* 157-168, 1988.

Peterson, L. C., Late Quaternary deep-water paleoceanography of the eastern Indian Ocean, 429 pp., Ph. D. thesis, Brown Univ., Providence, R. I., 1985.

Pichon, J. J., M. Labracherie, L. D. Labeyrie, and J. Duprat, Transfer functions between diatom assemblages and surface hydrology in the Southern Ocean, *Palaeogeogr. Palaeoclimatol. Palaeoecol., 61,* 79-96, 1987.

Platt, T., and G. Harrison, Biogenic fluxes of carbon and oxygen in the ocean, *Nature, 318,* 55-58, 1985.

Prell, W. L., and W. B. Curry, Faunal and isotopic indices of monsoonal upwelling: Western Arabian Sea, *Oceanol. Acta, 4,* 91-98, 1980.

Prell, W. L., J. Imbrie, D. G. Martinson, J. J. Morley, N. G. Pisias, N. J. Shackleton, and H. F. Streeter, Graphic correlation of oxygen isotope stratigraphy: Application to the late Quaternary, *Paleoceanography, 1,* 137-162, 1986.

Ramm, M., Karbonatsedimentasjon og senkvartaer paleo-oseanografi i det ϕstlige norskehavet: (siste 250.000 år), 161pp., pp., M. Sc. thesis, Inst. for Geologi, Univ. i Oslo, Norway, 1986.

Reimers, C. E., and E. Suess, Spatial and temporal patterns of organic matter

accumulation on the Peru continental margin, in *Coastal Upwelling, its Sediment Record,* Part B, edited by E. Suess and J. Thiede, pp., 311-346, Plenum, New York, 1983.

Romankevich, E. A., *Geochemistry of Organic Matter in the Ocean,* 343 pp., Springer-Verlag, Heidelberg, 1984.

Rowe, G. T., The biological fate of organic matter on the NE US continental margin-SEEP Area, 1983/84, *Eos Trans. AGU, 66 (18),* 283, 1985.

Sackett, W. M., W. R. Eckelmann, M. L. Bender and A. W. Bé, Temperature dependence of carbon isotope composition in marine plankton and sediments, *Science, 148,* 235-237, 1965.

Sarnthein, M., Zur Fluktuation der subtropischen Wüstengürtel seit dem letzten Hochglacial vor 18.000 Jahren: Klimahinweise und modelle aus Tiefseesedimenten, *Geomethodica, 7,* 125-161, 1982.

Sarnthein, M., J. Thiede, U. Pflaumann, H. Erlenkeuser, D. Fütterer, B. Koopmann, H. Lange, and E. Seibold, Atmospheric and oceanic circulation patterns off northwest Africa during the past 25 million years, in *Geology of the Northwest African Continental Margin,* edited by U. von Rad et al., pp. 545-604, Springer-Verlag, Heidelberg, 1982a.

Sarnthein, M., H. Erlenkeuser, and R. Zahn Termination I: The response of continental climate in the subtropics as recorded in deep-sea sediments, *Bull. Inst. Geol. Bassin Aquitaine, 31,* 393-407, 1982b.

Sarnthein, M. and R. Tiedemann, Towards a high-resolution stable isotope stratigraphy of the last 3.3 Million years, ODP Sites 658 and 659 off Northwest Africa, in *Proceedings ODP Leg 108,* vol. B, edited by W. Ruddiman, M. Sarnthein, J. Baldauf et al., U.S. Govt. Printing Office, Washington, (in press), 1988.

Sarnthein, M., K. Winn,and R. Zahn, Paleoproductivity of oceanic upwelling and the effect on atmospheric CO_2 and climatic change during deglaciation times, in *Abrupt Climatic Change, Proceedings of the NATO/NSF A. R. W. Symposium at Biviers/Grenoble 1985,* edited by W. H. Berger and L. D. Labeyrie, pp. 311-337, D. Reidel, Dordrecht, Holland, 1987.

Scholten, J. C., Ein Beitrag zur Geochemie und Sedimentations-geschichte am Carlsberg und Mittel-Indischen Rücken, 151 pp., Ph. D. thesis, Heidelberg Univ., Federal Republic of Germany, 1987.

Shackleton, N. J., Carbon-13 in *Uvigerina:* Tropical rainforest history in the equatorial Pacific carbonate dissolution cycles, in *The Fate of Fossil Fuel in the Oceans,* edited by N. R. Andersen and A. Malahoff, pp. 401-427, Plenum, New York, 1977.

Siegenthaler, U., and T. Wenk, Rapid atmospheric CO_2 variations and ocean circulation, *Nature, 308,* 624-626, 1984.

Stein, R., J. Rullkötter, and D. H. Welte, Accumulation of organic-carbon-rich sediments in the late Jurassic and Cretaceous Atlantic Ocean -A synthesis, *Chem. Geol., 56,* 1-32, 1986.

Stevenson, F. J., and C. N. Cheng, Organic Geochemistry of Argentine Basin sediments: carbon-nitrogen relationships and Quaternary correlations, *Geochim. Cosmochim. Acta, 36,* 653-671, 1972.

Suess, E., Particulate organic carbon flux in the oceans -Surface productivity and oxygen utilization, *Nature, 288,* 260-263, 1980.

Suess, E., and P. J. Müller, Productivity, sedimentation rate and sedimentary organic matter in the oceans, II, Elemental fractionation, Biogeochemie de la matiére organique à l'interface eau-sédiment marin, *Colloq. Int. CNRS 293,* pp. 17-26, Paris, France, 1980.

Sundquist, E. T., Geological perspectives on carbon dioxide and the carbon cycle, in *The Carbon Cycle and Atmospheric CO_2: Natural Variations Archean to Present, Geophys. Monogr. Ser.,* vol. 32, edited by E. T. Sundquist and W. S. Broecker, pp. 5-60, AGU, Washington D. C., 1985.

Sundquist, E. T. and W. S. Broecker, (eds.), *The Carbon Cycle and Atmospheric CO_2: Natural Variations Archean to Present, Geophys. Monogr. Ser.,* vol. 32, 627 pp., AGU, Washington D. C., 1985.

Takahashi, T., W. S. Broecker, and S. Langer, Redfield ratio based on chemical data from isopycnal surfaces, *J. Geophys. Res., 90,* 6907-6924, 1985.

Thiede, J., E. Suess, P. J. Müller, Late Quaternary fluxes of major sediment components to the sea floor at the northwest African continental slope, in *Geology of the Northwest African Continental Margin,* edited by U. von Rad et al., pp. 605-631, Springer-Verlag, Heidelberg, 1982.

Tomczak, M., Ausbreitung und Vermischung der Zentralwassermassen in den Tropengebieten der Ozeane, 1, Atlantischer Ozean, *Oceanol. Acta, 7,* 145-158, 1984.

Vincent, E., and W. H. Berger, Carbon dioxide and polar cooling in the Mio-

cene: the Monterey hypothesis, in *The Carbon Cycle and Atmospheric CO_2: Natural Variations Archean to Present, Geophys. Monogr. Ser.*, vol. 32, edited by E. T. Sundquist and W. S. Broecker, pp. 455-468, AGU, Washington D. C., 1985.

Vincent, E., and W. H. Berger, Timing of deglaciation from an oxygen isotope curve for Atlantic deep-sea sediments, *Nature, 314,* 156-158, 1986.

Walsh, J. J., G. T. Rowe, R. L. Iverson, and P. McRoy, Biological export of shelf carbon is a sink of the global CO_2 cycle, *Nature, 291,* 196-201, 1981.

Walsh, J., J. Dymond, and R. Collier, Rates of recycling of biogenic components of settling particles in the ocean derived from sediment trap experiments, *Deep Sea Res., 35,* 43-58, 1988.

Wefer, G., and J. S. Killingley, Carbon isotopes in organic matter from a benthic alga "Halimeda incrassata" (Bermuda): effects of light intensity, *Chem. Geol. Isotop. Geosci., 59,* 321-326, 1986.

Wefer, G., E. Suess, W. Balzer, G. Liebezeit, P. J. Müller, A. Ungerer, and W. Zenk, Fluxes of biogenic components from sediment trap deployment in circumpolar waters of the Drake Passage, *Nature, 299,* 145-147, 1982.

Wenk, T., and U. Siegenthaler, The high-latitude ocean as a control of atmospheric CO_2, in *The Carbon Cycle and Atmospheric CO_2: Natural Variations Archean to Present, Geophys. Monogr. Ser.*, vol. 32, edited by E. T. Sundquist and W. S. Broecker, pp. 185-194, AGU, Washington D. C., 1985.

Woodruff, F., S. M. Savin, and R. G. Douglas, Biological fractionation of oxygen and carbon isotopes by Recent foraminifera, *Mar. Micropaleontol., 5,* 3-11, 1980.

Zahn-Knoll, R., Spätquartäre Entwicklung von Küstenauftrieb und Tiefenwasserzirkulation im Nordost-Atlantik, Rekonstruktion anhand stabiler Isotope kalkschaliger Foraminiferen, Ph. D. thesis, 112 pp., Math. Naturw. Fakultät der Christian-Albrechts-Univ. Kiel, Federal Republic of Germany, 1986.

Zahn, R., K. Winn, and M. Sarnthein, Benthic foraminiferal $\delta^{13}C$ and accumulation rates of organic carbon: *Uvigerina peregrina* group and *Cibicidoides wuellerstorfi, Paleoceanography, 1,* 27-42, 1986.

Zahn, R., M. Sarnthein, and H. Erlenkeuser, Benthos isotopic evidence for changes of the Mediterranean outflow during the Late Quaternary, *Paleoceanography, 2,* 543-559, 1987.

J. C. Duplessy and M. R. Fontugne, Centre des Faibles Radioactivites, F-91190 Gif-sur-Yvette, France

M. Sarnthein and K. Winn, Geologisch-Paläontologisches Institut, Christian-Albrechts-Universität, D-2300 Kiel, Federal Republic of Germany.

(Received December 6, 1987;
revised April 7, 1988;
accepted April 13, 1988.)